NATIONAL AERONAUTICS AND SPACE ADMINISTRATION

Technical Memorandum 33-580

Estimating Weibull Parameters for Materials

E. Y. Robinson

JET PROPULSION LABORATORY
CALIFORNIA INSTITUTE OF TECHNOLOGY
PASADENA, CALIFORNIA

December 15, 1972

PREFACE

The work described in this report was performed by the Engineering Mechanics Division of the Jet Propulsion Laboratory.

CONTENTS

CONTENTS (contd)

TABLES

FIGURES

FIGURES (contd)

ABSTRACT

This paper deals with the statistical analysis of strength and fracture of materials in general, with application to fiber composites. The "weakest link" model is considered in a fairly general form, and the resulting equations are demonstrated by using a Weibull distribution for flaws. This distribution appears naturally in a variety of problems, and therefore additional attention is devoted to analysis and statistical estimation connected with this distribution. Special working charts are included to facilitate interpretation of observed data and estimation of parameters. Implications of the size effect are considered for various kinds of flaw distributions.

The paper describes failure and damage in a fiber-reinforced system. Some useful graphs are included for predicting the strength of such a system. Recent data on organic-fiber (PRD 49) composite material is analyzed by the Weibull distribution with the methods presented here. The contents should serve as a useful handbook for data characterization and statistical fracture analysis.

INTRODUCTION

The tensile strength of brittle materials is variable and usually low. As a result, a variety of statistical methods have been developed to aid in design of brittle structures under tensile loading.

The reinforcing materials used in resin-matrix composites are often brittle (e.g., boron, graphite, or glass filaments). The strength behavior of these filaments can be approached using the methods which have been traditionally applied to brittle materials.

There is abundant evidence to indicate that ultimate strength of any material is less variable if failure is preceded by plastic flow or microcracking, so that brittleness - where failure is not preceded by either - is inevitably accompanied by strength variability. The causes of this variability are many and varied and are related to both material factors and inherent testing problems.

At one time it was thought that imperfect experimental technique caused most of the specimen-to-specimen variation in laboratory measurements of strength of a brittle or complex material. However, development of new and sophisticated specimens and improved techniques has not been sufficient to eliminate the practical statistical problem, and gradually the need for statistically oriented experiments became more widely recognized.

In this paper some statistical models are reviewed for strength of a brittle material and the interpretation of test results in terms of the Weibull distribution. Some recent data on a fiber-composite material are used to illustrate the usefulness and potential limitations of a simple statistical interpretation.

I. STRENGTH OF MATERIAL WITH FLAWS

1. THE SIMPLE CHAIN OR SERIES MODEL

Variability of strength may be explained by the fact that materials inevitably contain a distribution of flaws of various severity, such as surface scratches, cracks at grain boundaries, inclusions, etc. Certain flaws may be characteristic of the specimen fabrication and handling process: for example, surface cracks introduced during machining. Such defects would be expected on the surface of the specimen. Other defects may be dependent only on length: e.g., chipping or spalling along sharp edges. Still other mechanisms may produce regions of severe local weakness throughout the material's volume, in which case the strength will be an inverse function of size, since flaws of varying severity are present and a smaller specimen is less likely to contain a sever flaw.

Whatever the distribution of the flaws, a basic assumption in predicting tensile strength of a brittle material is that, for a given stress, the worst flaw controls strength, just as the strength of a chain is controlled by the weakest link.

In fact, let's consider the statistical problem of a chain whose links have varying strengths. The weaker links can be thought of as representing material with more severe defects.

If the fraction $S(\sigma)$ of the links have strengths exceeding σ, then a chain composed of N links will successfully transmit the stress σ only if all its links survive. The probability that this occurs is the joint probability of N links surviving, namely S^N. The probability, G, that the chain fails (that is, that at least one link fails) is:

$$G = 1 - S^N. \qquad (1)$$

The number of links has an extremely strong effect on chain strength. This is shown schematically in Fig. 1 for a hypothetical link-strength distribution. This is an example of size effect.

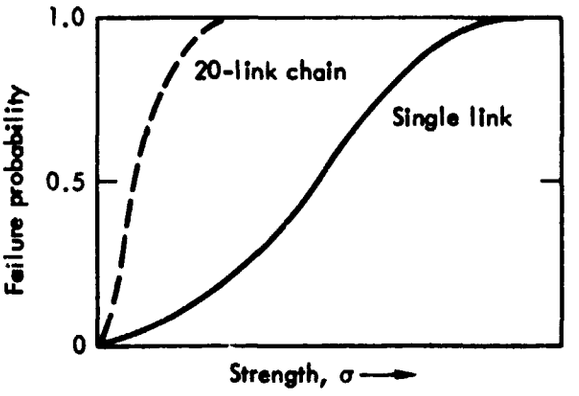

Fig. 1. Strength distribution for an individual link and a chain made of 20 such links.

The probability density distribution for single links and 20-link chains is the first derivative of the functions graphed in Fig. 1. These are depicted schematically in Fig. 2.

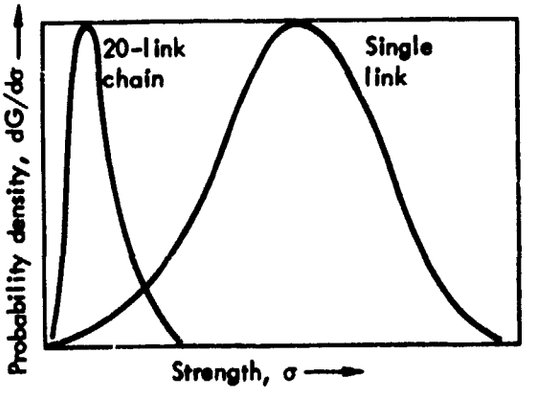

Fig. 2. Probability densities for the link and chain of Fig. 1.

In these two figures the curves for the chain represent the statistical behavior of the weakest of the 20 links, while the curves for the single link are based on the hypothetical link-strength distribution. We note in Fig. 2 that the chain (weakest link) distribution becomes distorted and less symmetric than the parent distribution.

The peaks of the curves in Fig. 2 represent the most probable values (modes) of the distributions, for which formulas may readily be developed. Using primes to denote differentiation with respect to strength, σ, the mode of strength is found by solving

$$\frac{d^2}{d\sigma^2}(1 - S^N) = 0,$$

which gives, for least value,

$$SS'' = -(N - 1)(S')^2. \qquad (2)$$

By similar arguments it may be shown that the most likely maximum value is a solution of

$$\frac{d^2}{d\sigma^2}\left[(1 - S)^N\right] = 0,$$

which gives

$$(1 - S)S'' = (N - 1)(S')^2. \qquad (3)$$

If an algebraic expression were put in for S these formulas would relate the modal extreme values of strength to the distribution size, N, and the distribution parameters in the function S.

For example, the link-strength distribution might be the Gaussian,

$$S = \int_t^\infty \frac{1}{\sqrt{2\pi}} e^{-t^2/2}\, dt = \text{erfc}(t),$$

whose derivatives are

$$S' = -\frac{1}{\sqrt{2\pi}} e^{-t^2/2} \text{ and } S'' = tS',$$

where t is the measure, in units of standard deviation, from the mean. The extreme values are given by

$$N = 1 + \sqrt{2\pi}\ |t|\ e^{t^2/2}\ \text{erfc}(t), \qquad (4)$$

where erfc(t) is the complementary error function defined above. Because of symmetry both modal extremes are estimated by Eq. (4). This equation, which predicts the most probable extreme value of t in a sample of size N, is graphed in Fig. 3.

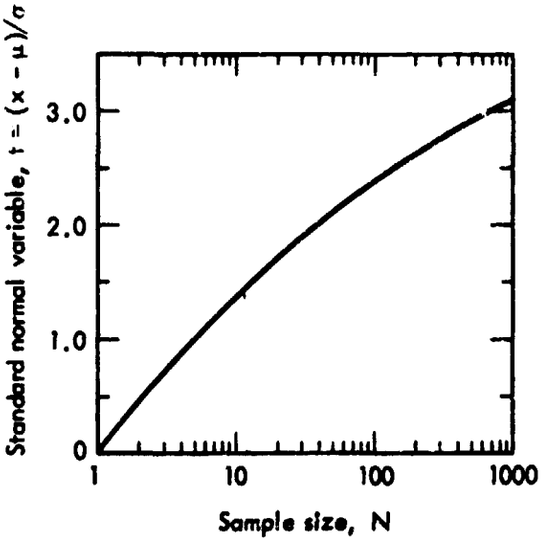

Fig. 3. Modal extremes of the standard normal distribution as a function of sample size.

When the form of the distribution S or S' is known and exhibits a mode, Eqs. (2) and (3) may be applied. There are, however, cases for which no mode exists (in the sense of Fig. 2 where the derivative vanishes),

and some alternative characteristic must be used to describe the chain strength. Take for example the simple exponential distribution

$$S = e^{-\lambda x}$$

for which the mean $\mu = 1/\lambda$. If Eq. (2) is applied here the result is not very useful. However, by applying Eq. (1) to find the mean value $\underline{x}$ of the least among N, we find

$$\underline{x} = \frac{\mu}{N} \quad \text{or} \quad \frac{\underline{x}}{\mu} = \frac{1}{N}.$$

The ratio of average chain strength to average link strength is thus seen to be inversely proportional to the number of links.

2. THE GENERAL CHAIN

It was tacitly assumed in the preceding section that all "links" in the chain model were loaded to the same stress, in analogy to a real chain. While this may be a practical model for filaments or whiskers, in a massive specimen of material there exist, inevitably, stress gradients caused by geometric features such as holes and other irregularities or as a result of intentionally applied moments. Localized failure will result from the most adverse combination of local stress and local weakness, so that it is not simply the weakest "link" which controls the initiation of fracture. We must, therefore, account for the variations in applied stress and the resultant effect on the local probability of failure.

The material is regarded as containing randomly situated local failure elements (links or flaws), with a strength distribution, $S(\sigma)$, expressing the probability that local strength

exceeds σ. Within a region ΔV_i where the density of failure elements (flaws) is ρ_i there exists a stress σ_i, and the probability that fracture does not initiate there is the probability that the number of failure elements which we expect in this volume will all simultaneously survive the stress σ_i. This joint probability is given by analogy with the simple chain:

$$S_i = \left[S(\sigma_i)\right]^{\rho_i \Delta V_i}. \qquad (5)$$

It should be noted that the number of flaws found in the volume ΔV_i is itself a statistical quantity and may be described by a Poisson distribution. This additional complication will be avoided by confining attention only to the expected number of flaws $\rho_i \Delta V_i$.

Extending Eq. (5) to consider additional volume elements making up a total volume V, we can write for the expected probability of joint survival S_V of all these regions:

$$S_V = \left[S(\sigma_1)\right]^{\rho_1 \Delta V_1} \left[S(\sigma_2)\right]^{\rho_2 \Delta V_2} \cdots$$

$$= \prod_{i=1}^{N} \left[S(\sigma_i)\right]^{\rho_i \Delta V_i}.$$

Taking logs gives the sum:

$$\ln S_V = \sum_{i=1}^{N} \rho_i \Delta V_i \ln \left[S(\sigma_i)\right].$$

By going to the respective limits of ΔV and N the sum may be replaced with the volume integral:

$$\ln S_V = \int_V \left[\rho \ln S(\sigma)\right] dV$$

or

$$S_V = \exp\left\{\int_V [\rho \ln S(\sigma)]\, dV\right\}. \quad (6)$$

In a fairly general way we have accounted for the nonuniform stress and the effect of volume, and, for good measure, we have allowed the flaw density to be space dependent. If the flaw strength distribution were known, as well as the flaw density and the applied stress, Eq. (6) could be used to predict the expected probability of survival of a specimen. Using

$$-\rho \ln S(\sigma) = g(\sigma)$$

we get

$$S_V = \exp\left[-\int_V g(\sigma)\, dV\right]. \quad (7)$$

The most convenient application of this equation is to assume tentative forms for the function $g(\sigma)$ and, if experimental results compare favorably, to utilize the assumed $g(\sigma)$ in analysis and design estimates. The well-known Weibull distribution results from putting

$$g(\sigma) = \left(\frac{\sigma}{\sigma_0}\right)^m.$$

B

II. ARRANGING AND PLOTTING STATISTICAL DATA

In the subsequent sections the interpretation of statistical data is considered in connection with estimating parameters and graphical depiction of the observations. Here, a short digression will be made to illustrate a method of assigning probabilities and plotting the data. The method described here is not unique, but it has been found convenient and reliable.

If a group of N observations of a variable x has been accumulated, the data should be arranged in serial order with increasing x and each of the observations numbered (ranked) in order. Now the question is: what probability does the jth observation represent? It should be clear, for example, that the smallest observation (rank j = 1) in a group of, say, ten ultimate strength measurements, should be plotted somewhere between 0 and 10% failure probability; and that the sixth of this group (rank j = 6) should be plotted between 50 and 60% failure probability. In general the jth observation should be plotted in the interval $(j-1)/N \leq F \leq j/N$. In fact, all plotting positions recommended in the literature fall in this interval. Obviously as N becomes large there will be little difference between (j-1)/N and j/N. According to this plotting method, no unique probability plotting position is selected. Instead a line, representing a probability interval, is drawn. The question of a unique plotting point has been the subject of some controversy, and various proposals have been made, for example:

$$F = \frac{j}{N}, \quad F = \frac{j-1}{N}, \quad F = \frac{j-1/2}{N},$$

$$F = \frac{j}{N+1}, \quad F = \frac{j-0.3}{N+0.4}.$$

The first two are, of course, the upper and lower bounds of the jth rank of length 1/N. The third form is the midpoint of the probability interval. The fourth is the so-called mean rank probability corresponding to the jth observation. The last expression is the median rank plotting position. Statistically this point divides the observations of the jth value into two equal groups. That is, if many samples of size N are taken, half of the jth observations are above and half below the variable corresponding with this value of probability. If a specific plotting position is desired, this one should be used. Finally, it is frequently useful to normalize the observed variables, using either the sample average or median as the normalizing factor. This allows samples having substantial differences in the variable but similar shapes to be studied jointly. This normalization is discussed in detail in subsequent sections.

An illustration of this method is given in Table 1 and Fig. 4. These are tensile strength data for glass filaments tested at $-196^{\circ}F$. The columns headed BAVG and BMED are normalized. In the summary at the bottom of the table CV is the ratio of standard deviation to the mean. The probability columns give the median rank plotting point, and the bounds of the probability interval. The plot of this data in Fig. 4 shows that the plotting point does not add much to interpretation or display of this sample. In later sections the problem of fitting such data with a theoretical distribution will be considered.

Table 1. Ranked sample data (column X) shown here are normalized to the mean and the median (columns BAVG and BMED, respectively). Plotting points and intervals are also shown.

GE E-GLASS SGL FIL -196 F REF AD 405697 1963

RANK J	X	BAVG	BMED	F-POINT (J-.3)/(N+.4)	F-INTERVAL J/N	RANK J
1	411.00000	0.50635	0.49222	0.02096	0.03030	1
2	578.00000	0.71209	0.69222	0.05090	0.06061	2
3	578.00000	0.71209	0.69222	0.08084	0.09091	3
4	588.00000	0.72441	0.70419	0.11078	0.12121	4
5	671.00000	0.82666	0.80359	0.14072	0.15152	5
6	701.00000	0.86362	0.83952	0.17066	0.18182	6
7	724.00000	0.89196	0.86707	0.20060	0.21212	7
8	748.00000	0.91537	0.88982	0.23054	0.24242	8
9	749.00000	0.92276	0.89701	0.26048	0.27273	9
10	754.00000	0.92892	0.90299	0.29042	0.30303	10
11	795.00000	0.97943	0.95210	0.32036	0.33333	11
12	800.00000	0.98559	0.95808	0.35030	0.36364	12
13	815.00000	1.00407	0.97605	0.38024	0.39394	13
14	827.00000	1.01885	0.99042	0.41018	0.42424	14
15	828.00000	1.02009	0.99162	0.44012	0.45455	15
16	833.00000	1.02625	0.99760	0.47006	0.48485	16
17	835.00000	1.02871	1.00000	0.50000	0.51515	17
18	842.00000	1.03733	1.00838	0.52994	0.54545	18
19	847.00000	1.04349	1.01437	0.55988	0.57576	19
20	847.00000	1.04349	1.01437	0.58982	0.60606	20
21	895.00000	1.10263	1.07186	0.61976	0.63636	21
22	900.00000	1.10879	1.07784	0.64970	0.66667	22
23	905.00000	1.11495	1.08383	0.67964	0.69697	23
24	912.00000	1.12357	1.09222	0.70958	0.72727	24
25	913.00000	1.12480	1.09341	0.73952	0.75758	25
26	915.00000	1.12727	1.09581	0.76946	0.78788	26
27	916.00000	1.12850	1.09701	0.79940	0.81818	27
28	920.00000	1.13343	1.10180	0.82934	0.84848	28
29	930.00000	1.14575	1.11377	0.85928	0.87879	29
30	936.00000	1.15314	1.12096	0.88922	0.90909	30
31	944.00000	1.16300	1.13054	0.91916	0.93939	31
32	960.00000	1.18271	1.14970	0.94910	0.96970	32
33	974.00000	1.19996	1.16647	0.97904	1.00000	33

AVERAGE = 811.69697
STD DEV = 131.00727
CV = 0.16140
MEDIAN = 835.00000

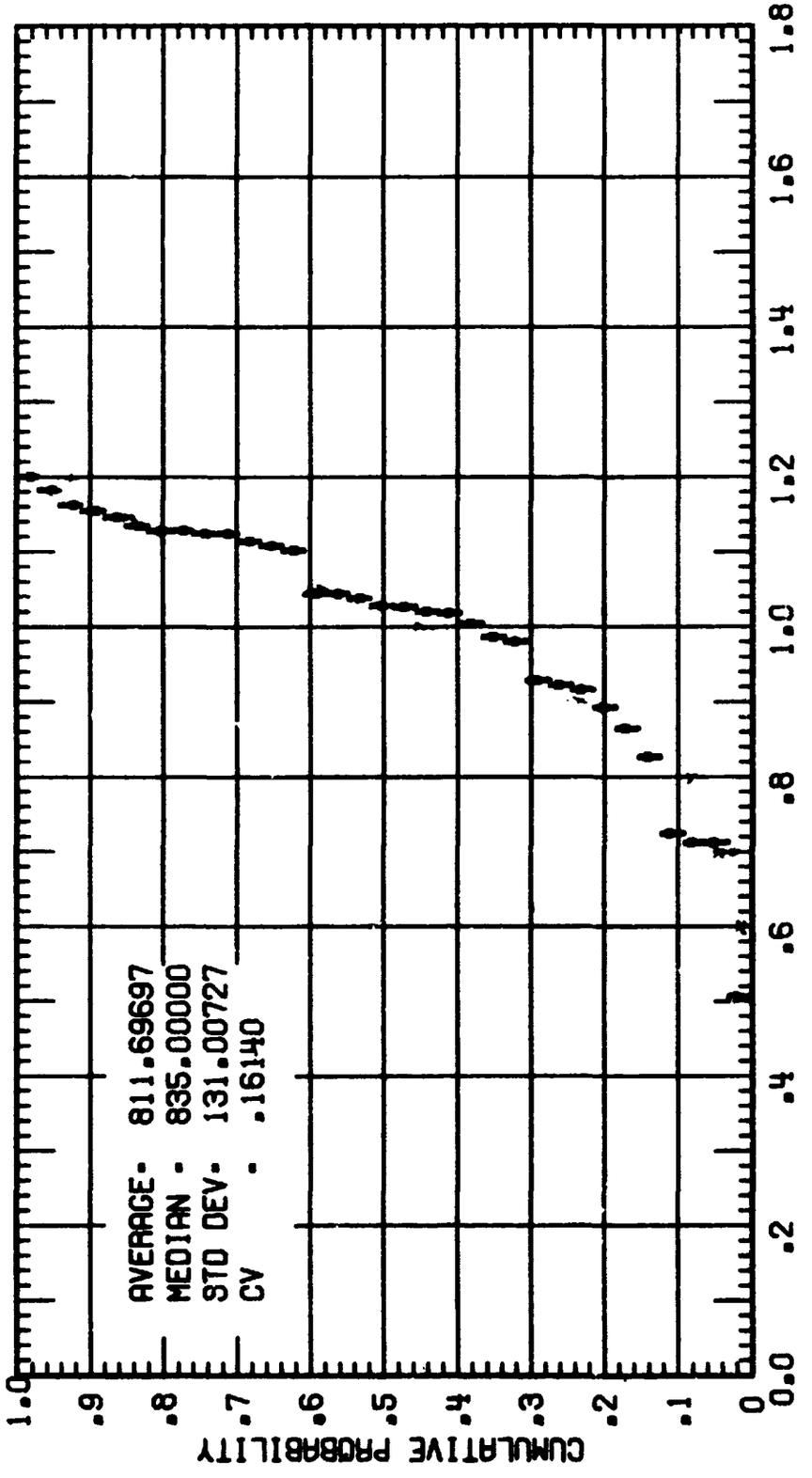

Fig. 4. Strength distribution of glass filaments (data from Table 1).

III. SOME PROPERTIES OF THE WEIBULL DISTRIBUTION

1. ANALYTICAL FORM

The conventional form of the so-called two-parameter Weibull distribution is:

$$S = \exp\left[-\int_V \left(\frac{\sigma}{\sigma_0}\right)^m dV\right] \qquad (8)$$

where S is the probability of survival, σ is an arbitrary applied stress in a volume V, and m and σ_0 are parameters.

To see the implication of this formula, consider a specimen under uniform, aniaxial tension. The specimen is assumed to fail according to the weakest-link model; that is, upon the initiation of fracture anywhere, gross failure occurs. If the stress is everywhere the same, Eq. (8) becomes

$$S = \exp\left[-\left(\frac{\sigma}{\sigma_0}\right)^m V\right]. \qquad (9)$$

This distribution is shown for V = 1 in Fig. 5. The variability decreases as m increases, and for low values of m, say less than 2, it becomes very obviously nonsymmetric. Below m = 1 there is no mode.

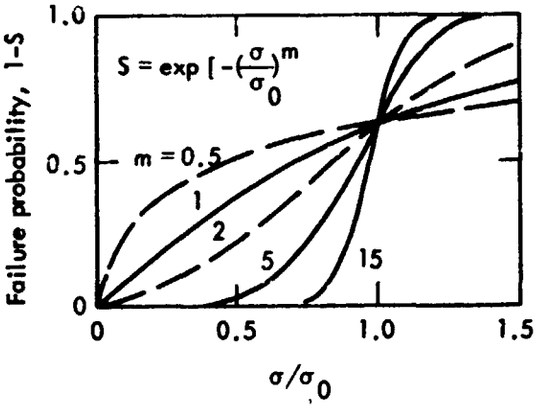

Fig. 5 Shapes of Weibull distributions.

One of the purposes of strength measurements on a particular material is to estimate the value of the modulus m for that material so as to characterize the material for structural reliability forecasts. Various analytical and graphical method of making such estimates will be discussed later.

In the case of flexural stress, a form different from Eq.(9) results. Using $\sigma = \sigma_B \left(\frac{y}{c}\right)\left(\frac{x}{s}\right)$ to describe the stress distribution in a simple centrally loaded rectangular beam (of half-height c, half-span s, and total volume V_B) we find

$$S = \exp\left[-\left(\frac{\sigma_B}{\sigma_0}\right)^m \frac{V_B}{2(m+1)^2}\right], \quad (10)$$

The change of stress distribution has introduced a factor affecting only the volume. The situation in simple bending is equivalent analytically to uniform tension provided appropriate correction is applied to the volume. This is a manifestation of the size effect, which is discussed next.

2. THE SIZE EFFECT

Large specimens of brittle or "weakest-link" material are weaker than small specimens, just as the long chain is weaker than the short one. If specimens of sizes V_1 and V_2 are tensile-tested and are characterized by similar values of m and σ_0, Eq. (9) may be used to compare the strength at the same probability of failure (when m and σ_0 are the same this also compares the mean strengths of both volumes), leading to

$$\sigma_1^m V_1 = \sigma_2^m V_2,$$

and the well-known strength size effect

$$\frac{\sigma_1}{\sigma_2} = \left(\frac{V_2}{V_1}\right)^{1/m}. \quad (11)$$

This equation immediately suggests a method for estimating m.

Rewriting it in logarithmic form gives

$$\log\left(\frac{\sigma_1}{\sigma_2}\right) = \frac{1}{m} \log\left(\frac{V_2}{V_1}\right),$$

and a plot of strength ratios vs volume ratios on logarithmic coordinates should yield a straight line of slope 1/m if the Weibull distribution is appropriate. In fact, Eq. (11) holds also for any stress distribution provided that the stresses applied to the various sized specimens are geometrically similar. As pointed out before, the effective size is altered by changing the stress distribution. To compare, for example, the case of uniform tension with simple bending, we use Eqs. (9) and (10) (with identifying subscripts) at equal probabilities, getting

$$\sigma_B^m \frac{V_B}{2(m+1)^2} = \sigma_T^m V_T,$$

and the ratio of strengths is

$$\frac{\sigma_B}{\sigma_T} = \left[\left(\frac{V_T}{V_B}\right) 2(m+1)^2\right]^{1/m}, \qquad (12)$$

showing flexural strength greater than tensile strength, especially for more variable material.

In a similar way the expected strengths in uniform bending, or tension, or any stress distribution, may be compared at equal probabilities of failure, simply by equating the corresponding exponential terms from Eq. (8).

We can express this size effect in a general way (for constant m and σ_0) as follows. The applied stress is written in terms of a reference stress (say the maximum tensile stress) and a geometric function which describes the stress distribution (as was done above for the simple beam), that is, $\sigma_i[f_i(V)]$. The exponential terms of Eq. (8) for two arbitrary cases being compared become

$$\sigma_1^m \int_{V_1} \left[f_1(V)\right]^m dV = \sigma_2^m \int_{V_2} \left[f_2(V)\right]^m dV,$$

and the general expression for size effect becomes

$$\frac{\sigma_1}{\sigma_2} = \left[\frac{\int_{V_2} \left[f_2(V)\right]^m dV}{\int_{V_1} \left[f_1(V)\right]^m dV}\right]^{1/m} \qquad (13)$$

So far the flaws in the material have been tacitly assumed to be distributed throughout the volume and the integrations have been carried throughout the specimen volume. The strength-controlling flaws may, however, be confined in many cases to the surface (e.g. in glass) or even to the edges, and along the length of reinforcing fibers. For these cases the form of the stress distribution and the region of integration are different. Let's reconsider, for example, the simple beam of width b with a surface distribution of flaws. The exponential term now becomes

$$\underbrace{\left(\frac{\sigma_B}{\sigma_0}\right)^m 2 \int_{x=0}^{s} \left(\frac{x}{s}\right)^m b\, dx}_{\text{the bottom beam surface}}$$

$$+ \underbrace{\left(\frac{\sigma_B}{\sigma_0}\right)^m 4 \int_{x=0}^{s} \int_{y=0}^{c} \left(\frac{x}{s}\right)^m \left(\frac{y}{c}\right)^m dx\, dy.}_{\text{the surface on vertical sides of the beam, subject to tension}}$$

This leads us to

$$\left(\frac{\sigma_B}{\sigma_0}\right)^m \left[\frac{A}{m+1} + \frac{B}{(m+1)^2}\right]$$

where A is the area of the bottom surface in tension and B the total area of the vertical surfaces in tension.

Equation (13) was used to calculate the size effects in tension, simple bending, and uniform bending for flaws distributed throughout the volume, area, or length. The resulting formulas are collected in Table 2.

The size effect helps to explain why, even in brittle materials, the influence of stress concentrations, at holes or notches, is not as great as would be expected from the theoretical stress concentration factor and a maximum stress failure criterion. The large theoretical stresses are operative in very small volumes within which the probability of finding weakness is greatly diminished.

3. STANDARDIZED FORMS OF THE WEIBULL DISTRIBUTION

Just as the application of the normal distribution is broadened and eased by use of a standard normalized variable, so also is the case with the Weibull distribution. Equation (8) is rewritten using a reference stress and geometric function for stress distribution and put into logarithmic form:

$$\ln \frac{1}{S} = \left(\frac{\sigma}{\sigma_0}\right)^m \int_V [f(V)]^m \, dV.$$

If the strength σ_p corresponds to the probability S_p (e.g., σ_p might be the median and $S_p = 0.5$), then the constant σ_0 is given by

$$\left(\frac{1}{\sigma_0}\right)^m \int_V [f(V)]^m \, dV = \frac{\ln\left(\frac{1}{S_p}\right)}{\sigma_p^m}$$

and may be eliminated from Eq. (8) to give a new, and flexible, normalized form:

$$S = \exp\left[-\left(\ln\frac{1}{S_p}\right)\left(\frac{\sigma}{\sigma_p}\right)^m\right]$$

$$= \exp\left[-\left(\ln\frac{1}{S_p}\right)\eta^m\right]. \qquad (14)$$

Table 2. Size effects for Weibull models. Flaws are assumed to be distributed throughout the material in the volume model, on the surface only in the surface model, and on the edges only in the edge model.

	Volume model[a]	Surface model[b]	Edge model[c]
I. Geometrically similar stress on different volumes	$\frac{\sigma_1}{\sigma_2} = \left(\frac{V_2}{V_1}\right)^{1/m}$	$\frac{\sigma_1}{\sigma_2} = \left[\frac{A_2 + \frac{B_2}{m+1}}{A_1 + \frac{B_1}{m+1}}\right]^{1/m}$	$\frac{\sigma_1}{\sigma_2} = \left(\frac{l_2}{l_1}\right)^{1/m}$
II. Uniform bending vs uniform tension	$\frac{\sigma_{UB}}{\sigma_T} = \left[2(m+1)\frac{V_T}{V_{UB}}\right]^{1/m}$	$\frac{\sigma_{UB}}{\sigma_T} = \left[\frac{A_T}{A_{UB} + \frac{B_{UD}}{m+1}}\right]^{1/m}$	$\frac{\sigma_{UB}}{\sigma_T} = \left(\frac{l_T}{l_{UB}}\right)^{1/m}$
III. Simple bending vs uniform tension	$\frac{\sigma_B}{\sigma_T} = \left[2(m+1)^2\frac{V_T}{V_B}\right]^{1/m}$	$\frac{\sigma_B}{\sigma_T} = \left[(m+1)\frac{A_T}{A_B + \frac{B_B}{m+1}}\right]^{1/m}$	$\frac{\sigma_B}{\sigma_T} = \left[(m+1)\frac{l_T}{l_B}\right]^{1/m}$
IV. Simple bending vs uniform bending	$\frac{\sigma_B}{\sigma_{UB}} = \left[(m+1)\frac{V_{UB}}{V_B}\right]^{1/m}$	$\frac{\sigma_B}{\sigma_{UB}} = \left[(m+1)\frac{A_{UB} + \frac{B_{UB}}{m+1}}{A_B + \frac{B_B}{m+1}}\right]^{1/m}$	$\frac{\sigma_B}{\sigma_{UB}} = \left[(m+1)\frac{l_{UB}}{l_B}\right]^{1/m}$

[a] The volume is the total specimen volume subject to the indicated stress.

[b] Rectangular beam. Area A is the bottom beam area subject to tension. Area B is the vertical beam surface subject to tension. Note that if the proportion of A to B is constant, the results of I and IV are similar to those of the volume model.

[c] The edge length l is total length subject to tensile stress only. Note that for a rectangular beam loaded in tension, l is twice what it would be if the beam were loaded in bending.

It can be shown that if σ_p is the mean value of the reference stress at fracture then

$$\ln\left(\frac{1}{S_p}\right) = \left[\Gamma\left(1 + \frac{1}{m}\right)\right]^m = \Gamma^m.$$

This result allows us to write the distributuion of Eq. (14) in terms of a mean-normalized variable:

$$S = \exp\left(-\beta^m \Gamma^m\right) \qquad (15)$$

where $\beta = \sigma/\sigma_{mean}$.

Alternatively it may be more convenient or desirable to normalize to the stress at some other probability (e.g., in an incomplete test in which only a fraction of the test specimens have been observed); for example, the median. For this case $S_p = 0.5$ and Eq. (14) becomes

$$S = \exp\left(-0.693\lambda^m\right) \qquad (16)$$

where $\lambda = \sigma/\sigma_{median}$.

Experience has shown that, by and large, Eqs. (15) and (16) will give adequate service. Both of these normalized forms of the Weibull distribution have been plotted onto useful working charts in Figs. 6 and 7.

The normalized form is independent of the detailed stress distribution and therefore allows, in principle, the pooling of diverse groups of test data, if each has been appropriately normalized. The scaling parameter σ_0 has been replaced by an estimate of the mean or median derived from the sample, and only m remains to be estimated in order to fit a set of observations with a Weibull function. Furthermore, the normalized form lends itself readily to analytical manipulation, for example to determination of the variance and statistical behavior of extreme values, discussed next.

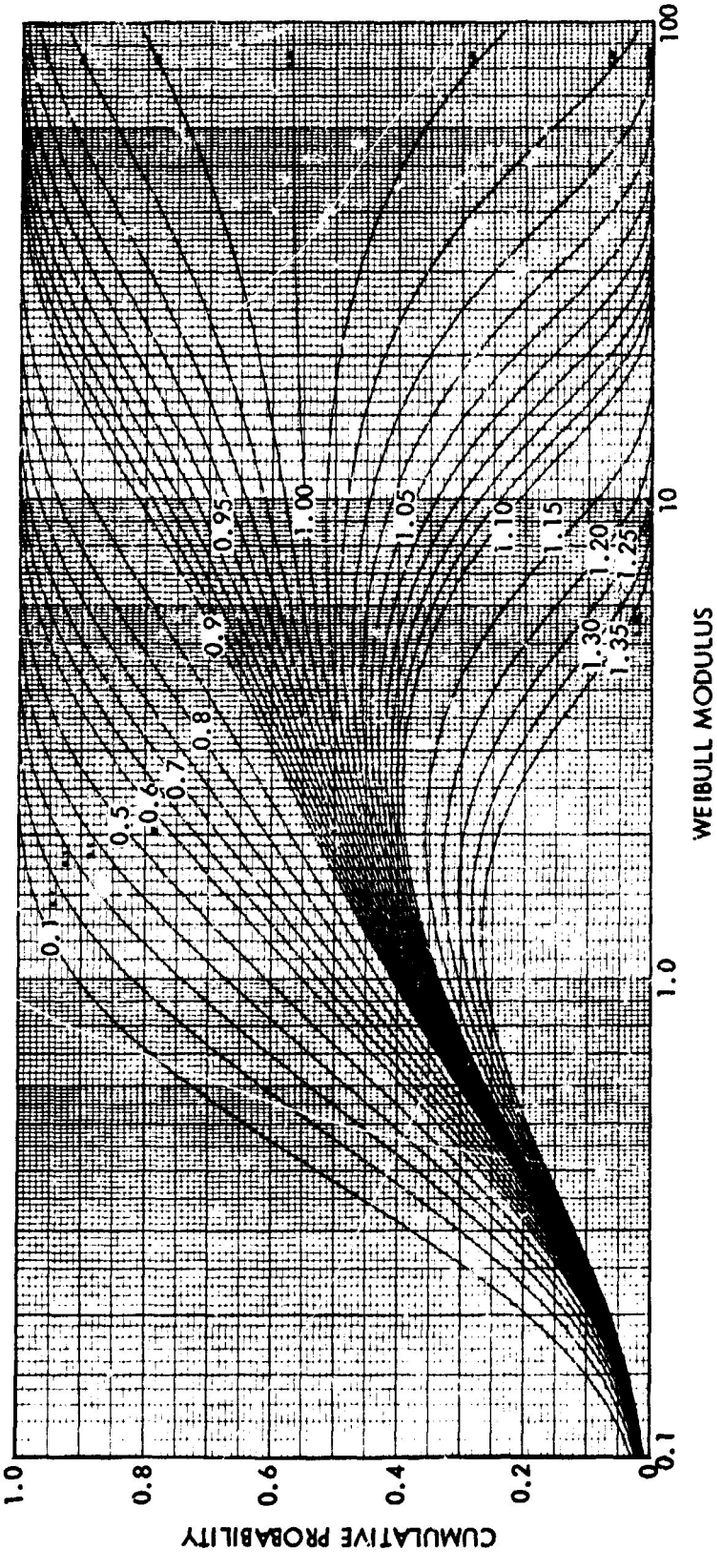

Fig. 6. Weibull distribution chart for variable normalized to mean.

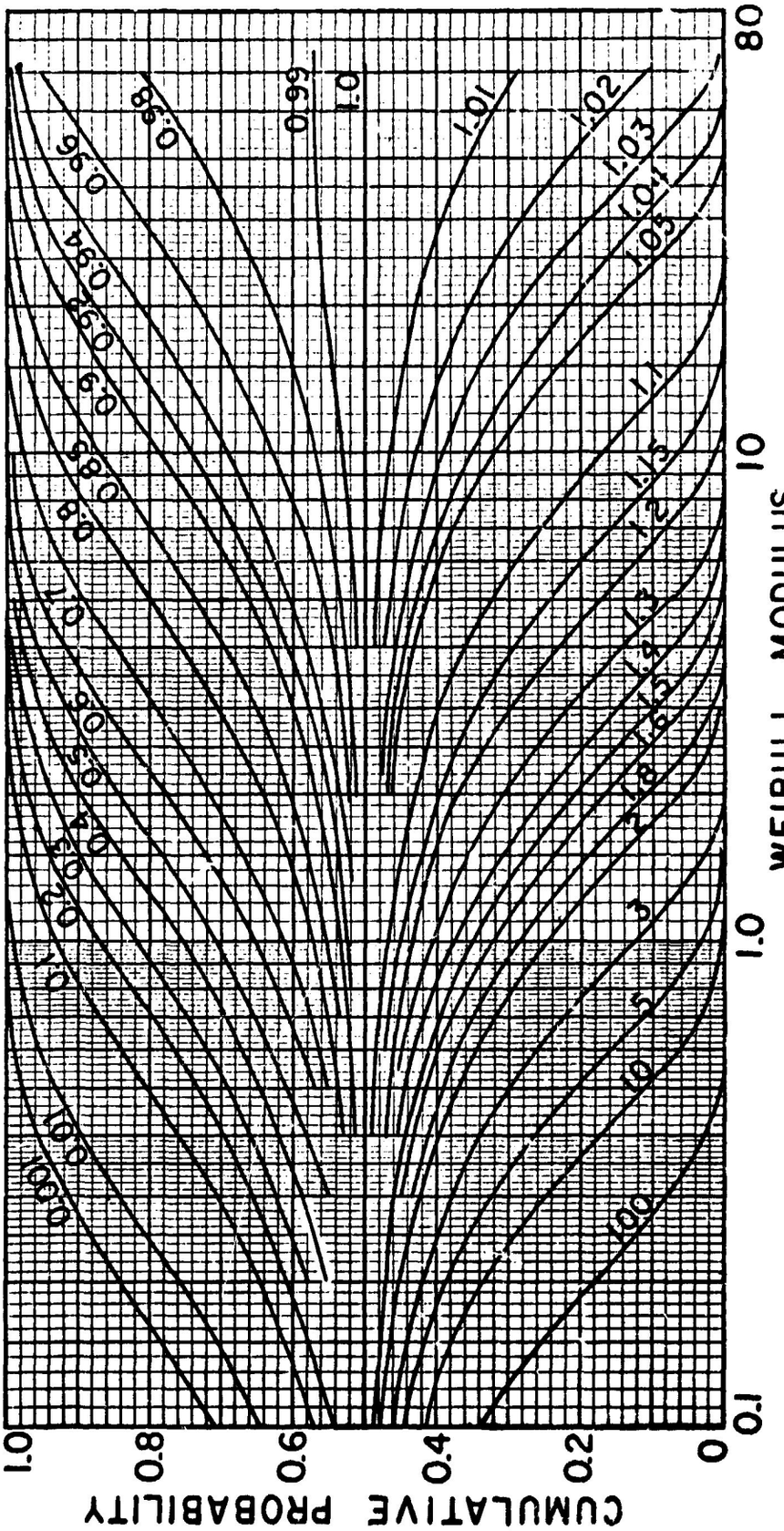

Fig. 7. Weibull distribution chart for variable normalized to median.

4. EXTREME VALUES OF THE WEIBULL DISTRIBUTION

Using the general formulas for extreme values given in Sec. I, we find the modal extremes of the normalized Weibull distribution η_{min} and η_{max}, to be given by

$$\eta_{min} = \left(\frac{m - 1}{mN \ln\frac{1}{S_p}}\right)^{1/m} \tag{17}$$

and

$$N = \left[1 - \frac{m - 1}{m\eta_{max}^{m} \ln\frac{1}{S_p}}\right] \left[\exp\left(\ln\frac{1}{S_p}\,\eta_{max}^{m}\right) - 1\right] + 1. \tag{18}$$

The modal range is determined from the difference between these extremes.

In figs. 8 and 9 are shown the extreme values and range, normalized to the mean. These charts give a useful perspective of the extreme-value behavior as sample size (or volume) increases. Equations (17) and (18) may be used to construct similar charts for median-normalized variables. A commonly used index of variability is the coefficient of variation CV defined as the ratio of standard deviation to sample mean.

We can easily calculate the coefficient of variation of the normalized Weibull distribution as well as the coefficient of variation of of the least values. The cumulative distribution of least values is, in accordance with Eq. (1):

$$G = 1 - S^N$$

$$= 1 - \exp\left[-N\left(\ln\frac{1}{S_p}\right)\eta^m\right].$$

The mean value of this distribution (the mean least value) is

$$\underline{\eta} = \int_0^\infty S_N \, d\eta = \frac{\Gamma(1 + 1/m)}{\left[N \ln\left(\frac{1}{S_p}\right)\right]^{1/m}}. \tag{19}$$

C

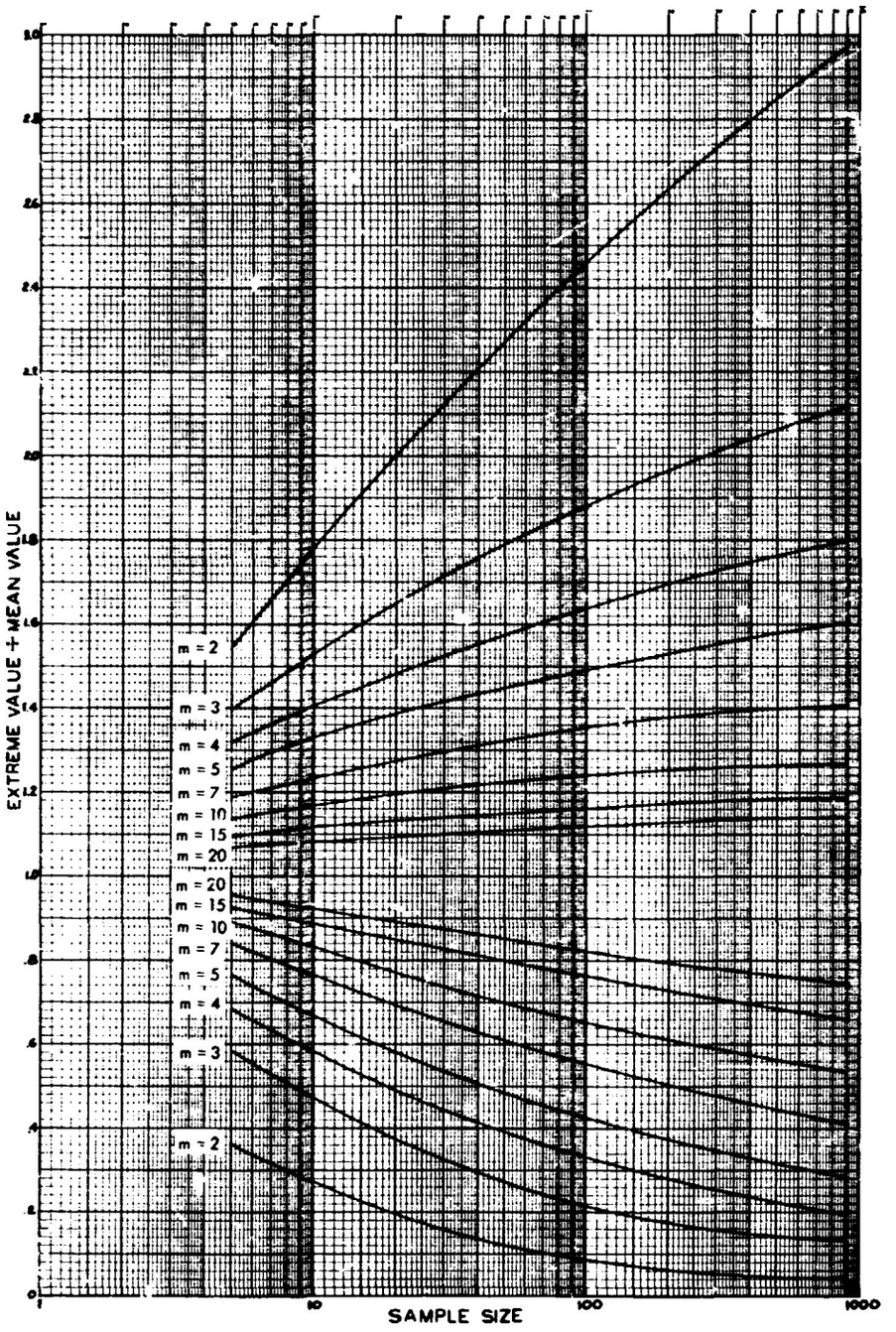

Fig. 8. Most probable extreme values of the Weibull distribution (relative to mean).

The formula for the variance is

$$\text{variance} = \int_0^\infty (\eta - \underline{\eta})^2 \left(-\frac{d\,S_N}{d\eta}\right) d\eta.$$

To carry out the integration it will be useful to employ the following integral formula:

$$H(p,c,m) = \int_0^\infty x^p e^{-cx^m}\,dx = \frac{\Gamma\left(1 + \frac{1+p}{m}\right)}{(1+p)\,c^{(1+p)/m}}.$$

The standard deviation of the least among N is found to be

$$\frac{1}{N^{1/m}} \sqrt{\frac{\Gamma(1 + 2/m) - [\Gamma(1 + 1/m)]^2}{\left[\ln\left(\frac{1}{S_p}\right)\right]^{2/m}}}. \quad (20)$$

The coefficient of variation for the Weibull distribution is obtained by combining Eqs. (19) and (20) and putting N = 1.

$$CV = \sqrt{\frac{\Gamma(1 + 2/m)}{[\Gamma(1 + 1/m)]^2} - 1}. \quad (21)$$

The standard deviation of the least values in a sample of size N may be compared with the sample mean or with the mean of the least values. The standard deviation of the least values relative to the sample mean is given by

$$CV = \frac{1}{N^{1/m}} \sqrt{\frac{\Gamma(1 + 2/m)}{[\Gamma(1 + 1/m)]^2} - 1},$$

while the coefficient of variation of the least values is the same as Eq. (21). Note in the last two equations that all reference to the normalizing term $\ln(1/S_p)$ has vanished. Equation (21) is graphed in Fig. 10 where two approximations are shown:

$$CV \approx \frac{1.2}{m} \text{ (a fair approximation)},$$

$$CV \approx \left(\frac{1}{m}\right)^{0.94} \text{ (an excellent approximation)}.$$

These approximations and the graph are handy for thumb-rule estimates.

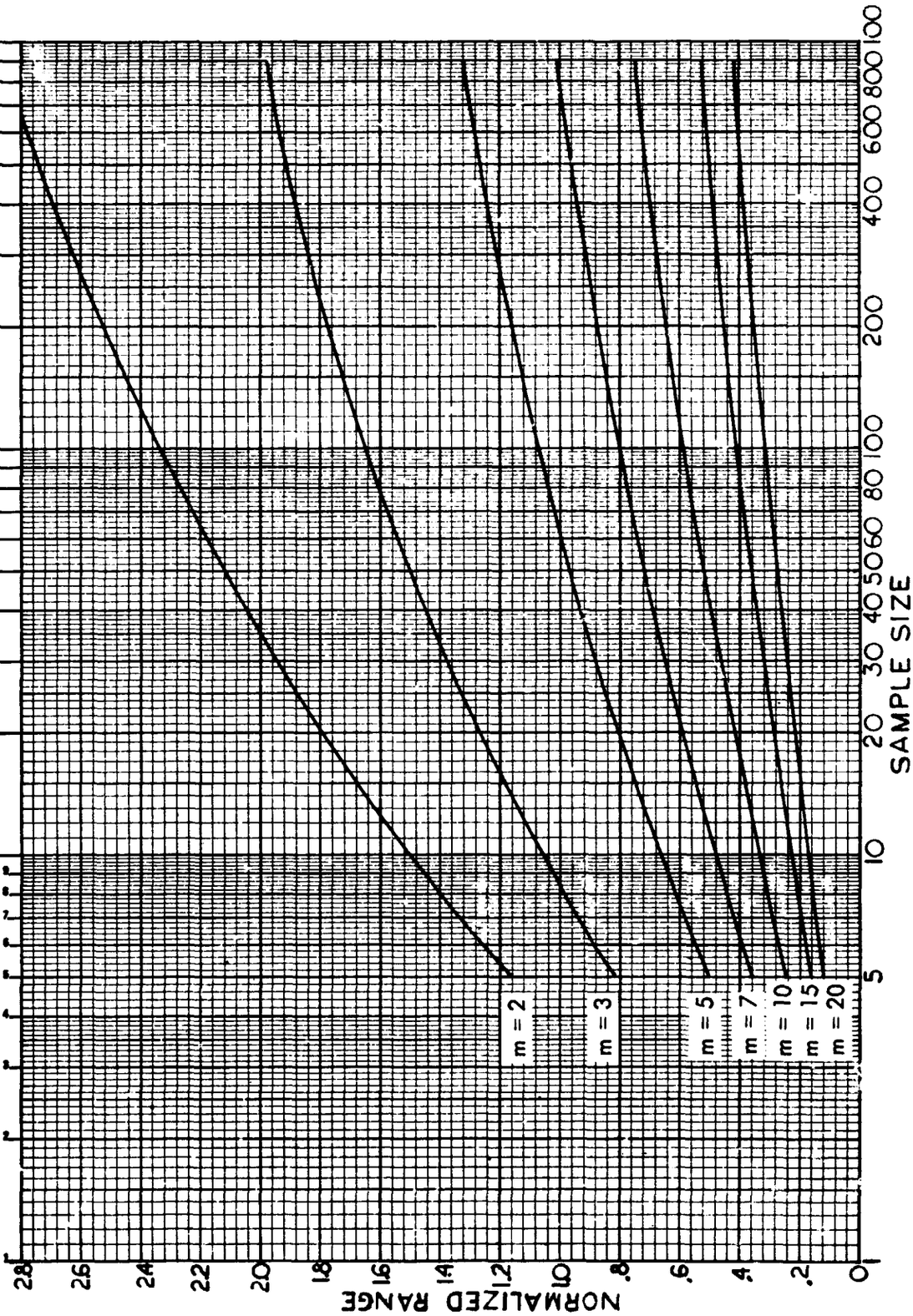

Fig. 9 Most probable range of the Weibull distribution (relative to mean).

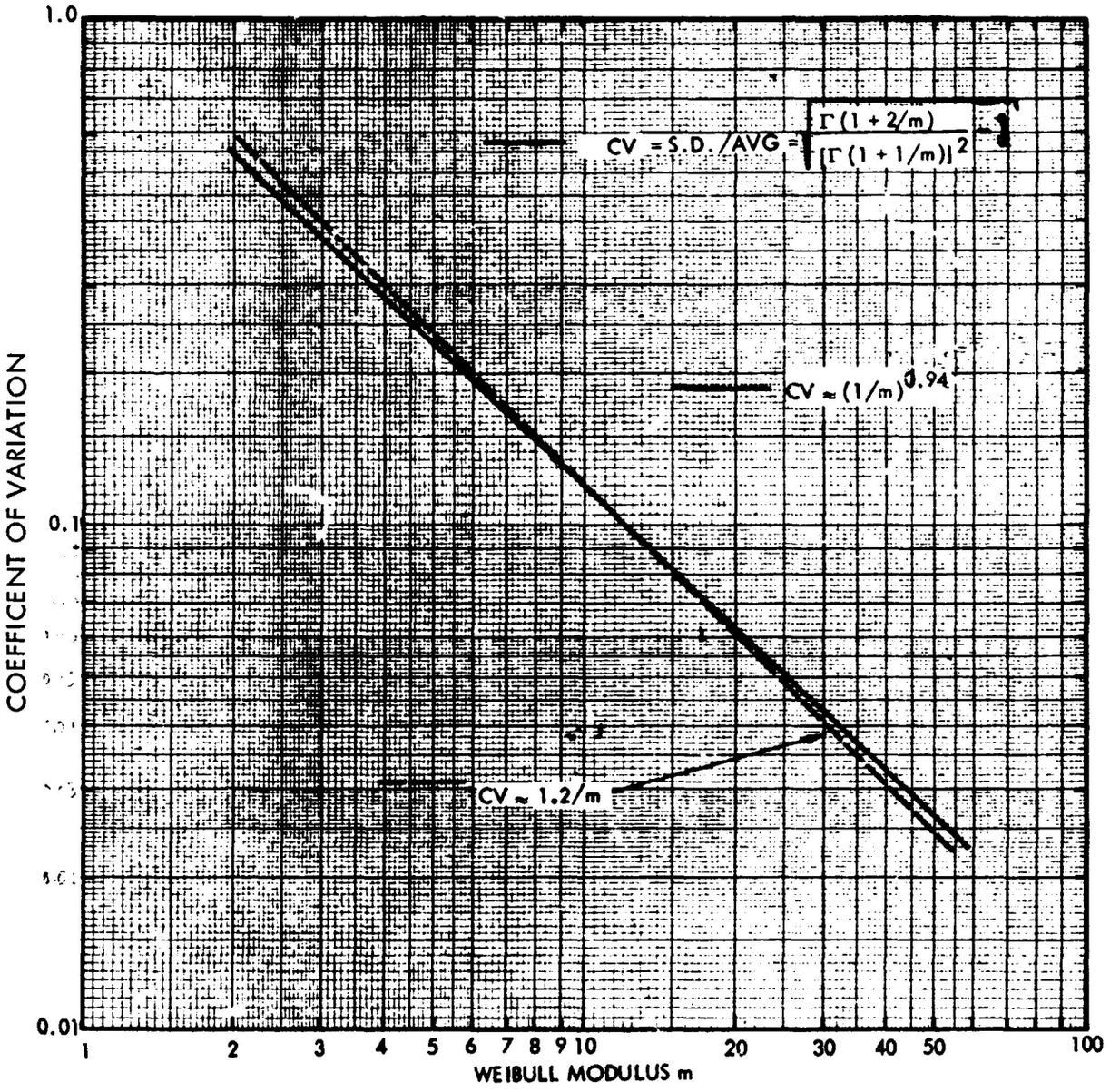

Fig. 10. Coefficient of variation (CV) vs Weibull modulus.

5. OTHER ESTIMATORS

There are, of course, many ways to estimate the parameters of a hypothetical distribution from the observed data. One of the more intriguing is the method of "maximum likelihood" which, in certain respects, would be expected to be at least as precise as, if not more precise than, any other estimator. Its application generally (the Weibull distribution included) requires an electronic computer, and therefore it may not be worth the effort if a computer is not readily available. In brief the method is as follows. If the probability density is $f(x,u_k)$ where the u_k are parameters of the distribution, a function is formed with the observations $x_1, x_2, x_3, \ldots, x_j, \ldots, x_N$ which is the simultaneous product of $f(x_j,u_k)$; that is, the joint probability density:

$$\Phi = \prod_{j=1}^{N} f(x_j,u_k).$$

Taking logs gives

$$ln\ \Phi = L = \sum_{j=1}^{N} f(x_j,u_k).$$

The maximum of this function, also called the "likelihood function," is sought by setting $\partial L/\partial u_k$ equal to zero:

$$\begin{aligned} \frac{\partial L}{\partial u_1} &= 0 = \sum_{j=1}^{N} \frac{\partial}{\partial u_1} f(x_j,u_k) \\ &\vdots \\ \frac{\partial L}{\partial u_k} &= 0 = \sum_{j=1}^{N} \frac{\partial}{\partial u_k} f(x_j,u_k). \end{aligned}$$

This gives k equations with k unknowns (the parameters u_k). If certain requirements are met by the function L, these equations may be solved for the u_k parameters. The parameters u_k computed this way are called maximum likelihood estimates.

Still another analytical approach is a point-by-point estimate of m, using each ranked observation separately, and finally combining these individual estimates in a weighted average to give the sample estimate. Using Eq. (14) and solving for m,

$$m = \frac{1}{\ln \eta} \ln\left[\frac{\ln(1/S)}{\ln(1/S_p)}\right].$$

The median rank plotting position for the jth observation η_j is

$$S_j = 1 - \frac{j - 0.3}{N + 0.4} = \frac{N - j + 0.7}{N + 0.4}.$$

Therefore the jth observation may be used to estimate m by

$$m_j = \frac{1}{\ln \eta_j} \ln\left[\frac{\ln\left(\frac{N + 0.4}{N - j + 0.7}\right)}{\ln(1/S_p)}\right].$$

Each of the j estimates of m should be weighted in accordance with the sensitivity of m to changes of S. Since the charts of Figs. 6 and 7 use coordinates of S and log m, a weighting factor for the graphical estimates is

$$w_j = \left|\frac{dS}{d(\ln m)}\right|.$$

That is, the steeper lines on the charts give more reliable estimates of m.

The formula for w_j becomes

$$w_j = \left(\ln\frac{1}{S_p}\right)(\ln \eta_j)\, m_j\, (\eta_j)^{m_j} \times \left\{\exp\left[-\left(\ln\frac{1}{S_p}\right)(\eta_j)^{m_j}\right]\right\}.$$

The m-estimate is the weighted average:

$$\hat{m} = \frac{\sum_{j=1}^{N} w_j m_j}{\sum_{j=1}^{N} w_j}.$$

6. HOW GOOD ARE THE m-ESTIMATES?

A broad answer to this question is -- not very! A study was made of the different methods of estimating m, using computer-generated samples drawn from known, controlled parent distributions. The following estimators were investigated:

1) Minimum value.

2) Maximum value.

3) Range.

4) Coefficient of variation.

5) Maximum likelihood.

6) Log-log graphical estimates (Fig. 11).

7) Semilog graphical estimates (Fig. 6).

No one method appeared consistently superior for the range of m-values (3-30) and sample sizes (10-100) studied. Broadly speaking, the estimates of m were normally distributed about the true value with a coefficient variation of $\sqrt{1/N}$. The results of the study are summarized in Fig. 11.

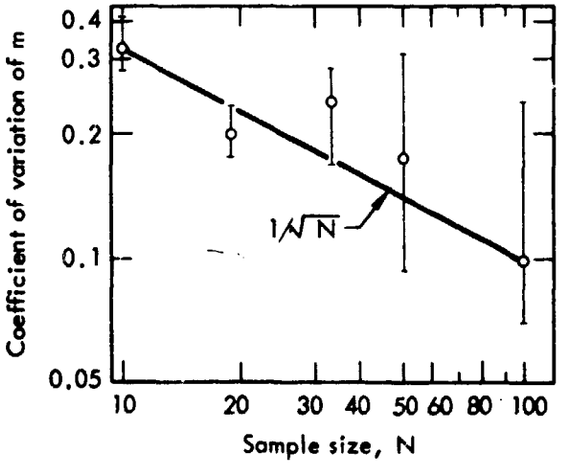

Fig. 11. Variability of m-estimators.

IV. ESTIMATING THE WEIBULL MODULUS, m, FROM OBSERVED DATA

After a set of data has been accumulated, say N observations of strength for brittle beams, it is possible to interpret the data and determine whether a Weibull distribution gives a good fit and what the best choice of the modulus m is to fit the observed data. Once the distribution is completely defined, it is possible to predict the strength of other structures of the same material operating under known stress distribution. It is also possible to make a straightforward determination of the probability of survival (reliability) for a given mass of the material under specified operational conditions. By this analysis the "safety factor" used in design can be directly related to the probability of survival.

Assuming the experimental data has been arranged and tabulated as described in Sec. II, a number of provisional estimates of m may be quickly made for thumb-rule purposes. The final choice should result from a graphical examination. Various m-estimates will now be described.

To illustrate the application of the various estimators, a sample of 10 observations was prepared, drawn at random from a parent population having a Weibull distribution with m = 6 and a mean of 1. Twenty samples of 10 each were actually drawn. The 20 least values (rank = 1) were averaged to give the first entry in Table 3. The 20 next-to-least values (rank = 2) were averaged to give the second entry, and so on. Thus, each of the table entries is an average of 20 values.

Table 3. Sample data for illustrating various methods of estimating the Weibull modulus m.

Rank, j	Fraction of mean	Fraction of median	Median rank plotting point, $\frac{j - 0.3}{N + 0.4}$	Probability interval
1	0.660	0.654	0.067	0-0.1
2	0.807	0.799	0.163	0.1-0.2
3	0.890	0.882	0.26	0.2-0.3
4	0.950	0.941	0.356	0.3-0.4
5	0.983	0.974	0.452	0.4-0.5
6	1.035	1.025	0.548	0.5-0.6
7	1.089	1.08	0.644	0.6-0.7
8	1.135	1.124	0.74	0.7-0.8
9	1.192	1.181	0.837	0.8-0.9
10	1.257	1.245	0.923	0.9-1.0

Statistical determinations:

Mean = 1.000

CV = 0.182*

Median = 1.009

*The value of CV for the sample is computed by

$$CV = \sqrt{\frac{\sum (x/\hat{\mu} - 1)^2}{N - 1}}$$

where $\hat{\mu}$ is the sample average and N the sample size.

1. SINGLE NUMBER ESTIMATES

All of the working charts presented in Sec. III may be used to estimate m from observed data. Figure 8, 9, and 10 are directly applied

with the observed extreme values, range, and coefficient of variation, respectively. The following estimates of m are obtained for the sample data in Table 3:

Basis of estimate	Graph used	Estimate of m
Maximum (1.257)	Fig. 8	6
Minimum (0.660)	Fig. 8	5
Range (0.597)	Fig. 9	5.5
CV (0.182)	Fig. 10	6.4

2. GRAPHICAL ESTIMATES

Recall Eq. (14) and write it in logarithmic form to get:

$$\log\left(\ln\frac{1}{S}\right) = m \log \eta + \log\left(\ln\frac{1}{S_p}\right). \quad (22)$$

On conventional log-log coordinates the data may be approximated with a straight line of slope m. In fact, such probability paper is available with suitably labeled coordinates, which eliminates the need to compute $\ln(1/S)$. Fig. 12 shows how this probability paper may be constructed. The slope of the straight line approximation may be measured directly to get an estimate of m. Figure 13 shows the sample data (from Table 3) plotted on this paper (both the probability plotting point and interval are shown), and the slope of a straight line fitted by eye to the data.

Charts of the normalized distributions (e.g., Figs. 6 and 7) are preferable to the log-log chart of Fig. 13 because they present the data in a more useful perspective. Therefore the data of Table 3 have been plotted in mean-normalized form in Fig. 14 and in median-normalized form in Fig. 15.

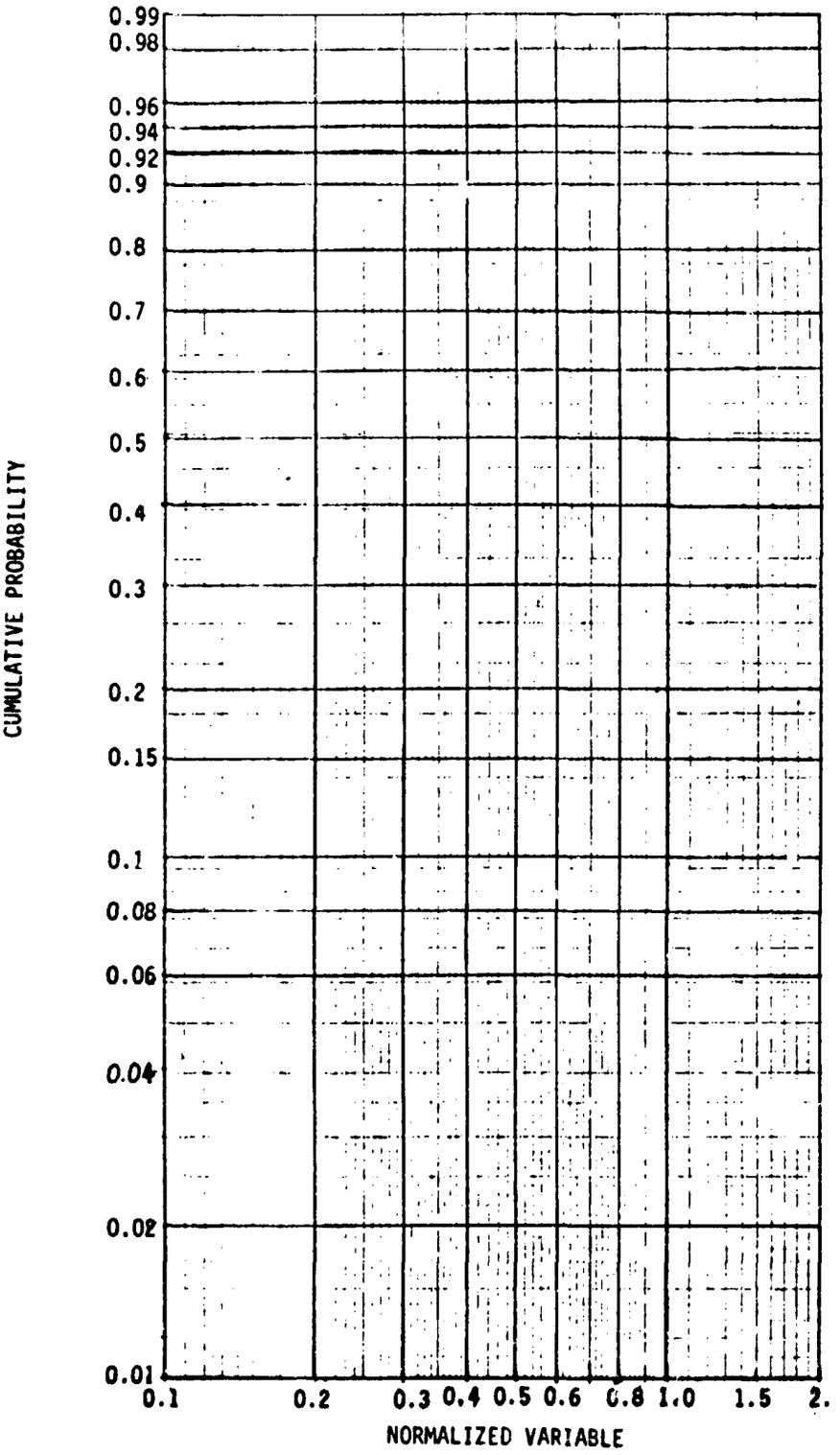

Fig. 12. Log-log Weibull probability paper.

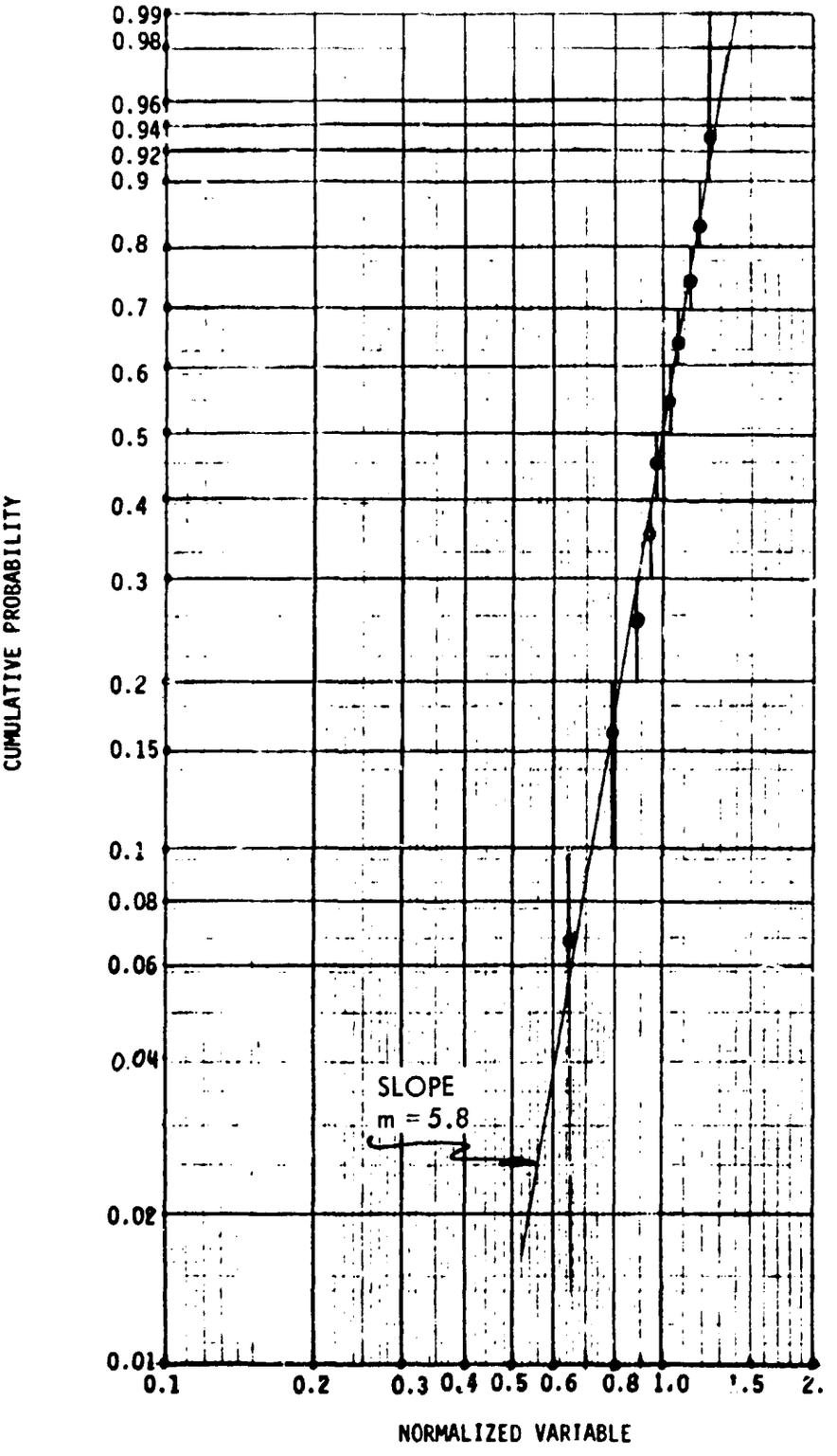

Fig. 13. Sample data on log-log paper.

PLOTTING POSITION = $\frac{r - 0.3}{N + 0.4}$

PROBABILITY INTERVAL = $\frac{1}{N}$

SAMPLE DATA

RANK	NORMALIZED VARIABLE	PLOTTING POSITION
1	0.6604	0.067
2	0.8073	0.163
3	0.8904	0.26
4	0.9501	0.356
5	0.9837	0.452
6	1.035	0.548
7	1.0897	0.644
8	1.1354	0.74
9	1.1926	0.837
10	1.2525	0.933

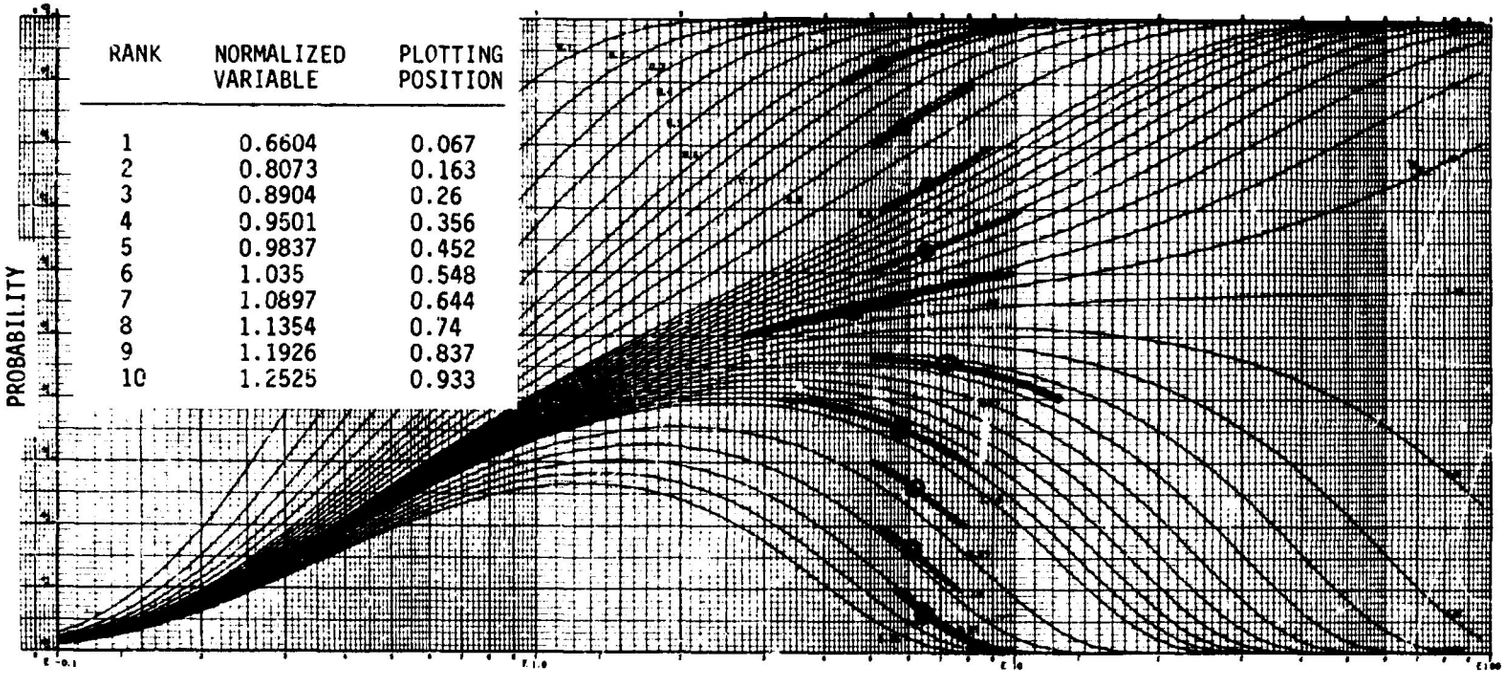

FIGURE A

EXAMPLE OF DATA ANALYSIS
SAMPLE DRAWN FROM A
PARENT POPULATION WITH M=6

Fig. 14. Sample data analysis using the mean-normalized variable.

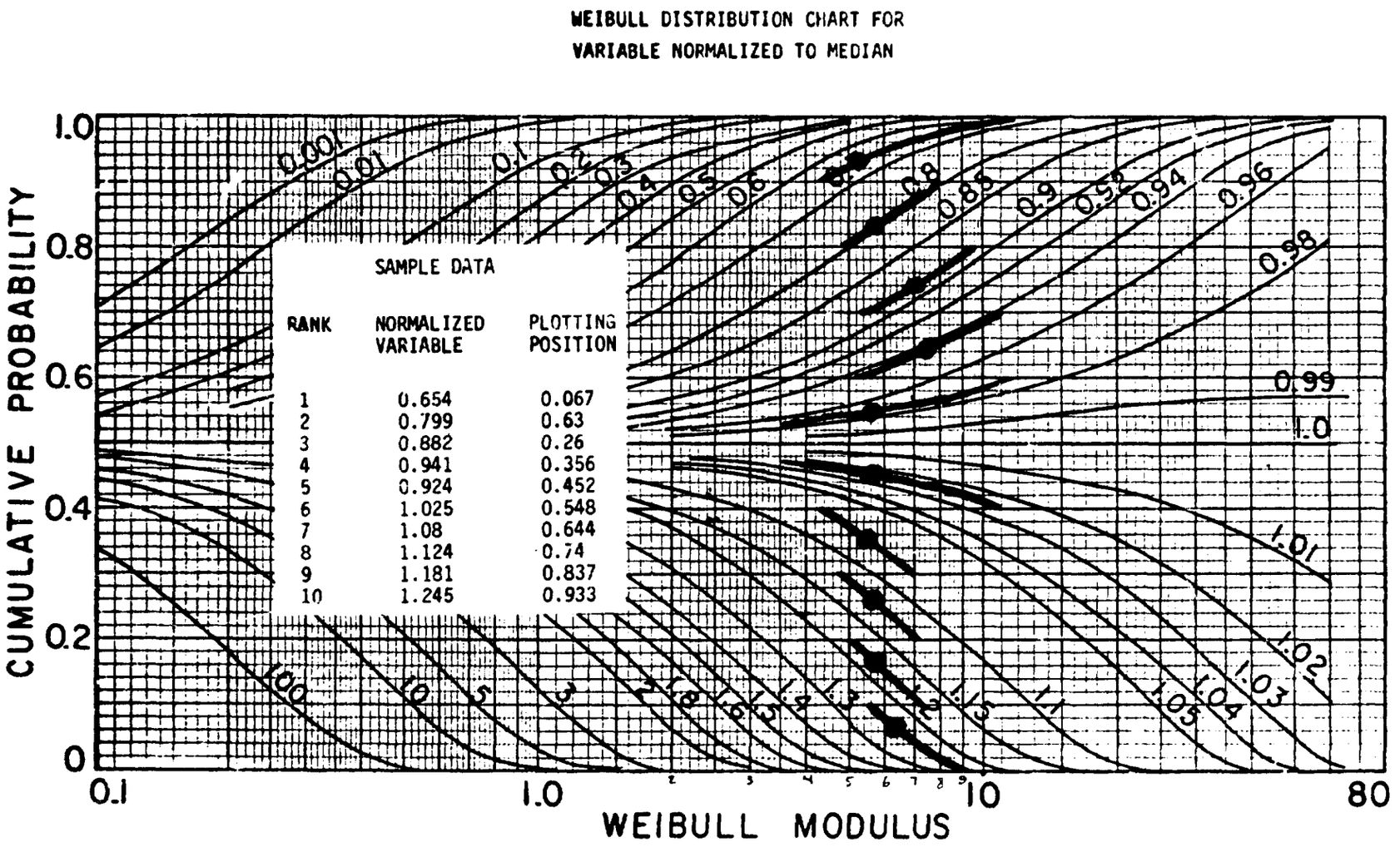

Fig. 15. Sample data analysis using the median-normalized variable.

These graphs show m = 6 to be an excellent fit to the data, and furthermore they give some information on the m-values represented in the sample.

In order to get a feeling for the way the approximation fits the sample data, a Cartesian plot was made using Fig. 14 as a basis. This plot, Fig. 16, exhibits a very satisfactory comparison between the observed data and the Weibull distribution with m = 6.

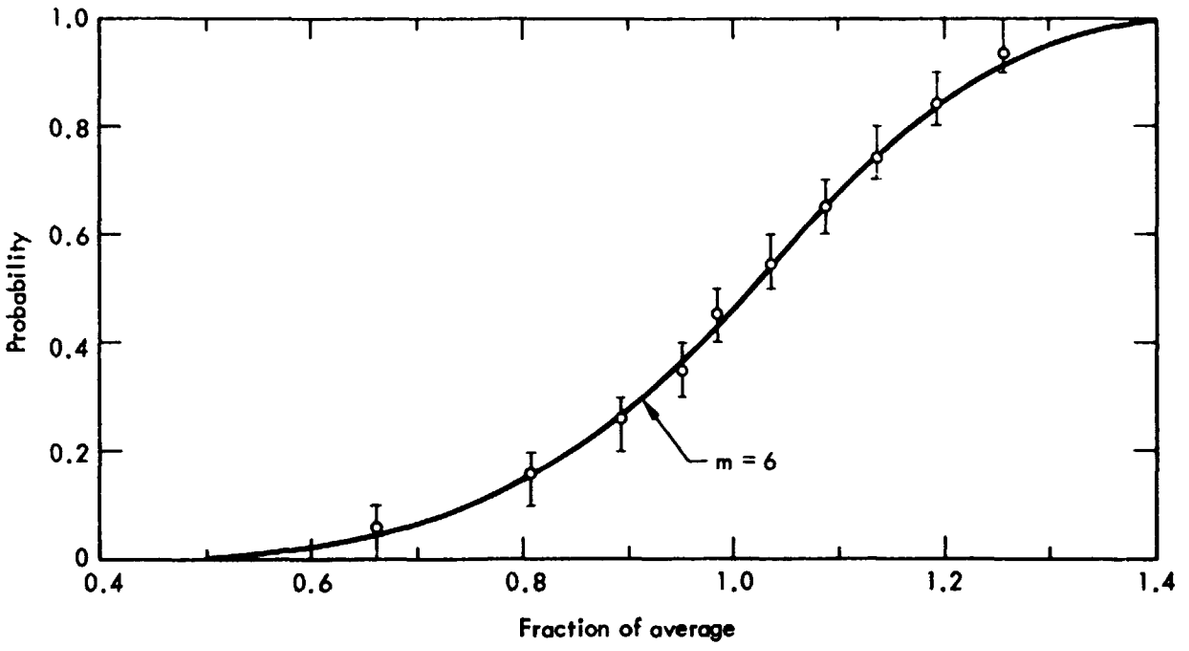

Fig. 16. Cartesian plot of sample data.

V. SOME COMMENTS ON APPLICATION

Is there any point in bothering with a statistical approach to brittle fracture when the methods of fracture mechanics are available to explain brittle fracture? After all, in principle, we need only know the geometry of the worst flaw in a structure and, from laboratory measurements of fracture toughness, we can predict the failure conditions. While the theoretical and experimental contributions of fracture mechanics have been substantial, a certain amount of caution must be exercised. Inspection of a structure for flaws involves some risk of passing over or missing a critical feature. Those flaws which are detected can be defined geometrically only within certain limits, and even repeated measurements on laboratory samples with controlled, artificially induced cracks exhibit a serious variability in fracture toughness.

A particularly striking example of fracture toughness variability is shown in Fig. 17. If we can assume that the material was carefully selected and the laboratory precracking of specimens was carefully controlled, the cause of this variability must be ascribed to statistically varying material properties.

Application of data such as that shown in Fig. 17 will require consideration of size, since more samples or a larger structure will increase the probability of experiencing a value of fracture toughness even less than observed in laboratory tests.

Conventional fracture mechanics does not account for this size effect. The following dramatic example will illustrate the point.*

---

*J. E. Srawley and J. B. Esgar, Lewis Research Center, Cleveland, Ohio, Rept. NASA-TM-X-1194 (Jan. 1966).

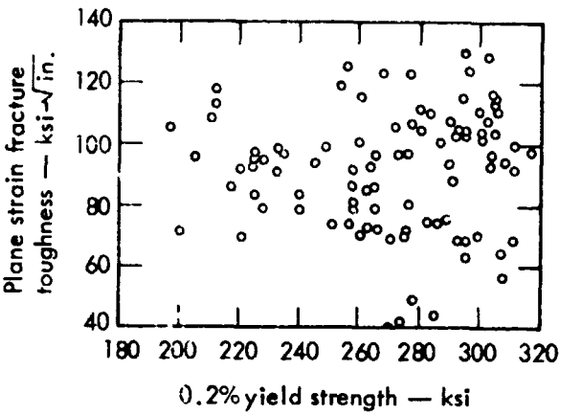

Fig. 17. Plane strain fracture toughness of 18% nickel maraging steels. (From W. F. Brown and J. E. Srawley, Plane Strain Crack Toughness Testing of High Strength Metallic Materials, ASTM-STP-410, 1966.)

In April of 1965, a 260-inch diameter rocket motor case failed during hydro-testing, at 56% of the intended proof pressure. Fracture emanated from a flaw in a weld. Analysis of the flaw indicated that the apparent fracture toughness was 57,000 psi-$\sqrt{\text{in}}$. Laboratory tests of a few precracked weld specimens gave the results shown in Table 4.

In the report, some comment is made regarding the discrepancy between the average fracture toughness of the laboratory specimens and the considerably lower fracture toughness of the operational structure. However, testing only 2 in. of weld out of a total of 1000 ft. of weld length requires statistical accounting for the effect of size. In view of the limited sample size estimates are necessarily going to be rough.

Using the observed value of CV with Fig. 10 we find m = 25. If the laboratory test samples can be considered to be representative of the

Table 4. Results of fracture toughness tests on five weld samples, each 2/8 by 3/8 in. in cross section, out of a total of 1000 ft of weld. (Data from NASA TM-X-1194)

Specimen No.	Fracture toughness, psi-$\sqrt{\text{in.}}$
1	77,700
2	77,500
3	75,400
4	84,500
5	75,000
Mean =	78,020
Std. dev. =	3,820
CV =	0.049

weld in the motor case, then the size effect will be given by Eq. (11):

$$\frac{K_{\text{motor case}}}{K_{\text{sample}}} = \left(\frac{V_{\text{sample}}}{V_{\text{motor case}}}\right)^{1/25} .$$

If we substitute in this equation the experimentally determined value for K_{sample}, 78,020 psi- in., and the ratio of sample size to total weld size, 2 in./12,000 in. or 1/6000, we obtain

$$K_{\text{motor case}} = 78{,}020(1/6000)^{1/25}$$

$$= 55{,}090 \text{ psi-}\sqrt{\text{in.}} .$$

Therefore, the fracture toughness exhibited by the worst region in the weld is, for us, no surprise. The coincidence of the worst flaw with the weakest region should also be anticipated since thermal-stress induced

flaws and effects of shock or partial loading will be most detrimental in the inferior region.

Actually there are three factors, all of them fundamentally statistical, which must be considered in evaluating the capacity of an operational structure. First is the distribution of "fracture toughness," presumed to be a material property. Second is the inherent distribution of flaw intensities in the fabricated structure (a low flaw intensity located in a region of low toughness may be critical). Third is the number of flaws and their spatial disposition. If all three factors are accounted for, a statement of reliability under specific operational conditions can be made. Conditions or materials which result in time-dependent changes can greatly complicate the problem. Examples of these are corrosive environments which cause sharpening and intensification of flaws, or physical changes in the material resulting in lowered fracture toughness, or gross geometric effects resulting from flow or corrosion which substantially alter the nominal stress field.

In designing an operational structure made of massive brittle material there is a strong motivation to employ only statically determinate supports, to allow precise calculation of stresses. However, since brittle materials are frequently quite strong in compression, it may be better in certain circumstances to give up detailed knowledge of the working stresses, in exchange for redundant support and "crack-tolerant" behavior. A simple example is shown in Fig. 18 comparing alumina (Al_2O_3) beams tested in simple flexure and as redundant beams with built-in ends. With redundancy the first tensile fractures are not

Redundant-Support Tests

Behavior comparison tests were made on three sizes of alumina beams, using the fixture shown at right to produce redundant end moments. All specimens were machined from a single slab of green-fired alumina (Wesgo Al-300) and fired simultaneously. Behavior of each size tested (example figure, below) shows good reproducibility. Results of these tests on redundantly supported beams, and on simply supported beams, are listed in the table below.

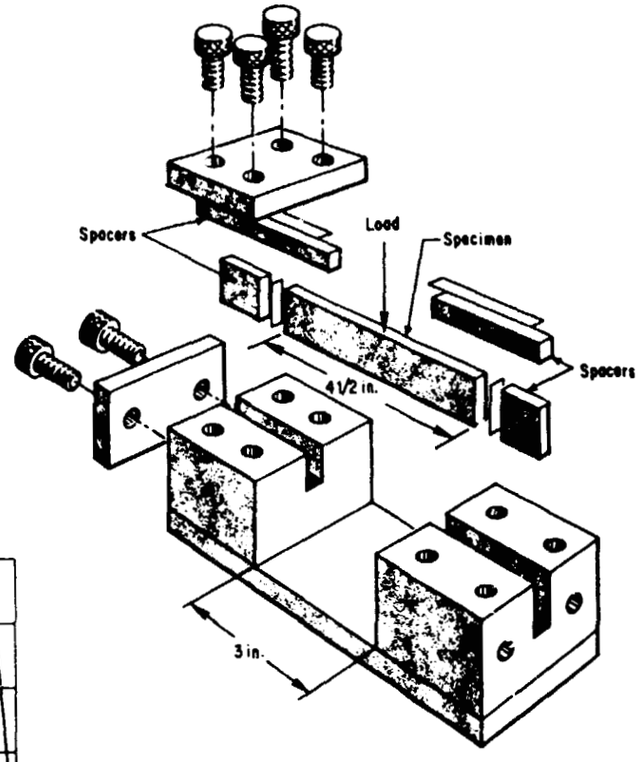

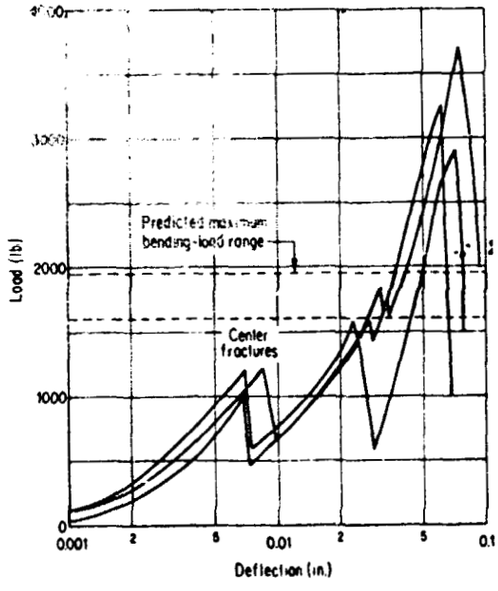

Fracture-Test Results on Simple and Fixed-End Beams

Specimen Size (in.)	Maximum Load (lb)	Predicted* Failure Load (lb)	—First Fracture— Load (lb)	—First Fracture— Deflection (in.)	Ultimate Fracture Load (lb)	Ultimate Fracture Deflection (in.)
	Simply Supported Beams		Fixed-End (redundant) Beams			
¼ x ¼	106	212	125	0.0040	245	0.057
			155	0.0045	280	0.058
¼ x ½	350	600	480	0.0040	600	0.1901
	302	to	800	0.0055	1140	0.090
		700	580	0.0055	1140	0.090
¼ x ¾	800	1600	1000	0.0070	2700	0.075
	980	to	1080	0.0085	3200	0.075
		1960	1090	0.0070	3250	0.085

*Predicted from simple-beam results, but under fixed-end conditions
†Loose end constraints

Fig. 18. Redundant support tests

followed by collapse - instead an archlike stability develops and eventual compressive failure of the segments is the cause of the collapse. The load-carrying capability of the redundant structure is substantially higher.

While some so-called brittle materials may be fairly well described by the "weakest link" or series model, it is abundantly clear that this

description of material failure is too severe. Even the most "brittle" materials demonstrate capacities for partial and multiple fracture, so that redundancy for load transmission is inevitably present, and it is only when such redundancy is exhausted that the weakest link decides collapse.

VI. APPLICATIONS TO MULTIFILAMENT STRANDS AND COMPOSITES

1. BRITTLE REINFORCING FILAMENTS

There is a rapidly growing interest in filament-reinforced structures. Small-diameter filaments and single-crystal whiskers currently being made exhibit very high strengths, in certain cases substantially above 10^6 psi. These are highly perfect structures, having fewer and less severe flaws than massive specimens of the same material. Such filaments are combined to form strands which may be woven into cloth or incorporated as non-woven layers in a structural composite. Massive structures are obtained with superior properties in certain directions. Filament winding is another means of producing strong lightweight structures. One of the most common reinforcing materials is the brittle material, glass. In fact, most high-strength reinforcing materials are brittle (e.g., graphite, boron, beryllium, etc.). We may, therefore, interpret the strength of single filaments according to the statistical methods developed in the previous sections, and extend the analysis to predict the strength of a multifilament strand. In doing so, one must be cautious about applying the frequently used "law of mixtures" to estimate strength. This "law" states that the strength of a composite is the weighted average of the stresses at failure in the constituents. That is, if the filaments in a composite exhibit a mean strength σ_f and occupy a volume or area fraction V_f, while at the filment failure strain ϵ_f the matrix carries the stress $E_m \epsilon_f$ in the remaining region $1 - V_f$, the composite strength will be

$$\sigma_c = \sigma_f V_f + \sigma_f \frac{E_m}{E_f}(1 - V_f) .$$

We will show that, inevitably, the "law of mixtures" should overestimate strength of an ideal multifilament strand. Translation efficiencies frequently quoted for composites are predicated on the erroneous assumption that the filament bundle should display a strength equal to the average of its constituents.

2. FAILURE PROCESS IN AN IDEAL STRAND

Assume a group of equally loaded filaments with a unique Young's modulus, with no interactions between filaments (that is, no shear coupling such as would result from twist, friction, or a binder), and independent failure wherein the failure of any filament does not precipitate immediate adjacent failure or alteration of the uniform loading among the surviving filaments. Take, for example, a strand made of 10 filaments with strengths ranked as shown in Table 5.

At what load would an ideal bundle of these filaments fail? Since the filaments are uniformly loaded, when the unit load (load per filament) exceeds 6.1 the weakest filament fails. This would occur at a total load of (6.1)(10) = 61. The load in the nine surviving intact filaments would then be 61/9 = 6.78, and at this load no further filament failure would occur.

When the nine survivors are subject to a unit load of 7.4, the next filament would fail. This is a total load of (7.4)(9) = 66.6 The unit load in the eight survivors would be 66.8/8 = 8.32, and no further fracture would follow.

The next filament would fail at a unit load of 8.5 or a total load of 8.5(8) = 68.0. The unit load in the seven remaining filaments would be 68/7 = 9.7; since this exceeds the strength of the next weakest

Table 5. Ranked strengths of individual filaments in an ideal strand of 10 filaments, to illustrate breaking behavior. Remaining capacity at any time is the total load on the strand required to break the weakest unbroken filament remaining.

Rank	Filament strength	Inverse rank	Remaining capacity
1	6.1	10	61
2	7.4	9	66.6
3	8.5	8	68*
4	9.2	7	64.4
5	10.1	6	60.6
6	10.6	5	53
7	11.0	4	44
8	11.6	3	34.8
9	12.3	2	24.6
10	13.2	1	13.2
Mean = 10.0			

*Overall maximum (bundle capacity).

filament, it would fail also, causing the unit load in the six remaining filaments to rise to 68/6 = 11.3. This, too, exceeds the strength of the next weakest filament and, following the next failure, the unit load rises to 68/5 = 13.6. Another filament snaps, leaving four filaments the weakest of which has a strength 11.0, and clearly our rope is done for - unless the load is reduced.

The last four filaments, for example, could sustain (11.0)(4) = 44 before the weakest among them failed. In summary, we discover that this ideal bundle has a maximum nominal unit capacity of 6.8 whereas the average strength of the constituent filaments is 10.0, and thus we were able to achieve ideally only 68% of the average strength that would have been predicted by the "law of mixtures."

The third column in Table 5 contains the inverse ranks of the filaments, which facilitate the computation of bundle capacity. The remaining bundle capacity is simply the product of the filament strength and its inverse rank. Note that for the data shown here (Sample 1), the bundle capacity rises monotonically to a maximum and then decreases monotonically to the last (and strongest) filament.

Another set of data (Sample 2) is shown in Table 6. Here the filament strengths are quite widely scattered and produce a series of local maxima of the remaining bundle capacity. When loaded, this particular bundle would exhibit partial breaking at 61, 68, and 70, and ultimate failure at 75 with only three filaments still intact. Here the nominal unit load at failure (7.5) is less than half of the average filament strength. The strength distributions of the Case 1 and Case 2 filament samples and the bundle capacities are plotted in Fig. 19.

Table 6. Breaking behavior of a 10-filament strand with filament strength distribution different from that in Table 5.

Filament strength	Inverse rank	Remaining capacity
6.1	10	61*
6.5	9	58.5
8.5	8	68*
9.2	7	64.4
11.5	6	66.3
14	5	70*
15	4	60
25	3	75**
30	2	60
32	1	32
15.8 (mean)		

*Local maximum.
**Overall maximum (bundle capacity).

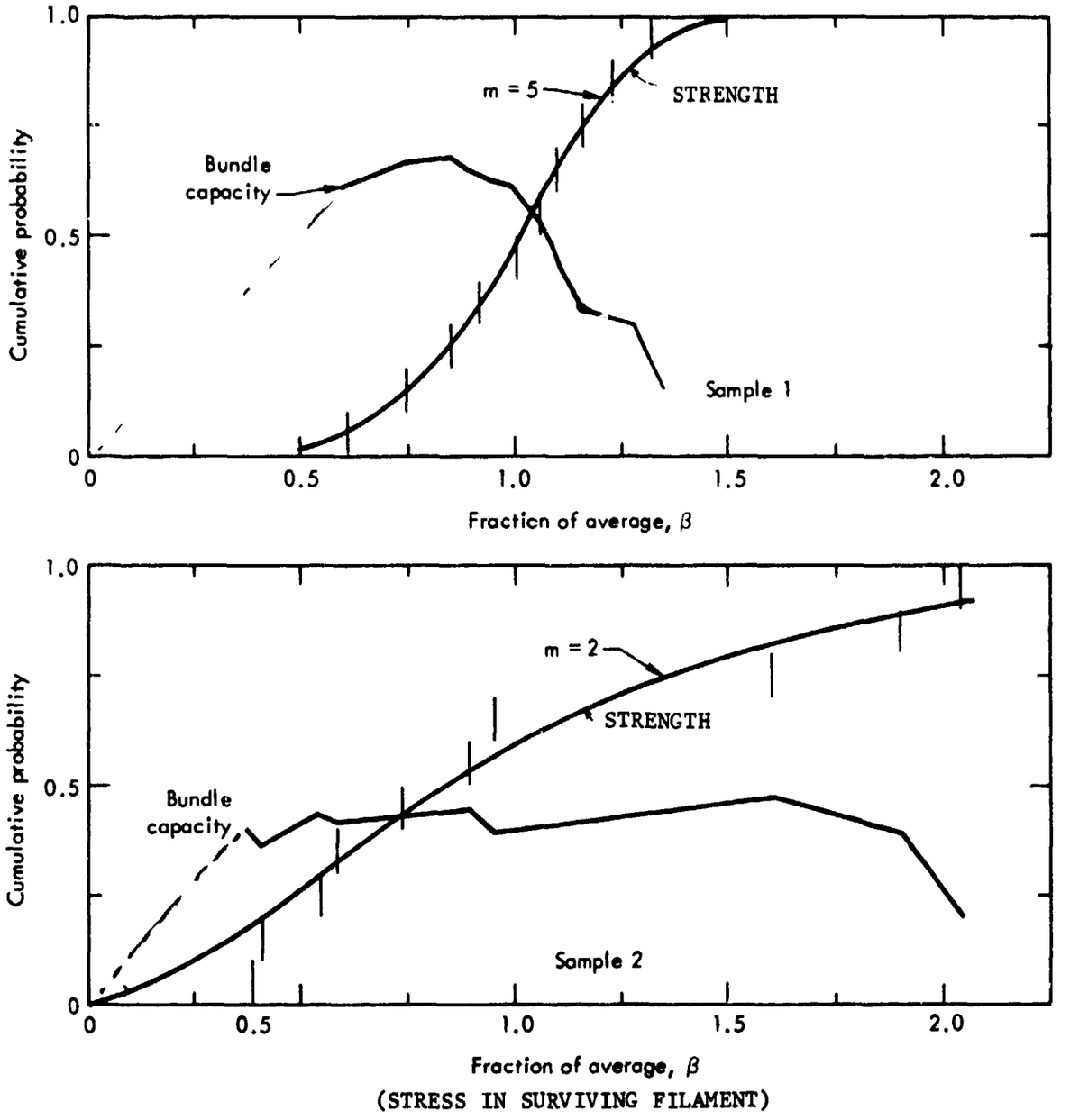

Fig. 19. Plots of individual filament strength and bundle capacity (data from Tables 5 and 6).

3. ANALYSIS OF IDEAL UNIFORMLY LOADED FREE STRANDS

If $S(\sigma)$ is the upper rank strength distribution for filaments (that is, S is the probability that strength exceeds σ), the nominal stress in a bundle wherein the applied unit stress is σ will be

$$\sigma_{nom} = \sigma\, S(\sigma). \qquad (23)$$

Here S is analogous to the "inverse rank" in the previous example, and σ is the strength of the weakest filament still intact. The bundle's capacity is the maximum value σ_{nom} may achieve. We find this by setting its derivative with respect to σ equal to zero:

$$\frac{d\sigma_{nom}}{d\sigma} = \sigma S' + S = 0$$

The solution of this equation will be the maximum stress achieved in the filaments, σ_*,

$$\sigma_* = -\frac{S}{S'}, \qquad (24)$$

and the nominal bundle strength will be

$$\sigma_{nom} = \sigma_* S(\sigma_*), \qquad (25)$$

or, in normalized terms,

$$\eta_{nom} = \eta_* S(\eta_*).$$

Various choices for the strength distribution may be made to explore the trends of formula (23). Let us take, for example, the Weibull distribution of Eq. (14), repeated below:

$$S = \exp\left[-\left(\ln\frac{1}{S_p}\right)\eta^m\right] \qquad (26)$$

Then the solution of Eq. (25) gives

$$\eta_* = \left[\frac{1}{m\left(\ln\frac{1}{S_p}\right)}\right]^{1/m}. \qquad (27)$$

The fraction remaining intact at this maximum stress is $S(\eta_*)$,

$$S(\eta_*) = \exp\left(-\frac{1}{m}\right), \tag{28}$$

and the nominal bundle strength becomes

$$\eta_{nom} = \left[\frac{1}{me\left(\ln\frac{1}{S_p}\right)}\right]^{1/m}. \tag{29}$$

Recalling that for the mean-normalized Weibull distribution,

$$\ln\frac{1}{S_p} = \left[\Gamma\left(1 + \frac{1}{m}\right)\right]^m = \Gamma^m$$

we find

$$\beta_{nom} = \left(\frac{1}{me}\right)^{1/m}\frac{1}{\Gamma} \quad \text{and} \quad \beta_* = \left(\frac{1}{m}\right)^{1/m}\frac{1}{\Gamma} \tag{30}$$

These formulas give the maximum stress achieved in the filaments and the expected nominal strength of an ideal, uniformly loaded, strand. These are graphed in Fig. 20, which shows that, even with about 5% std. dev. ($m \approx 25$), the nominal bundle strength only achieves 85% of the filament average.

In many cases formula (30) can be applied as a practical estimate of composite strength.

If the composite is carefully fabricated, with the proper choice of matrix, its strength will exceed predictions based on the free-strand formulas above; however, misalignment, nonuniform loading, filament

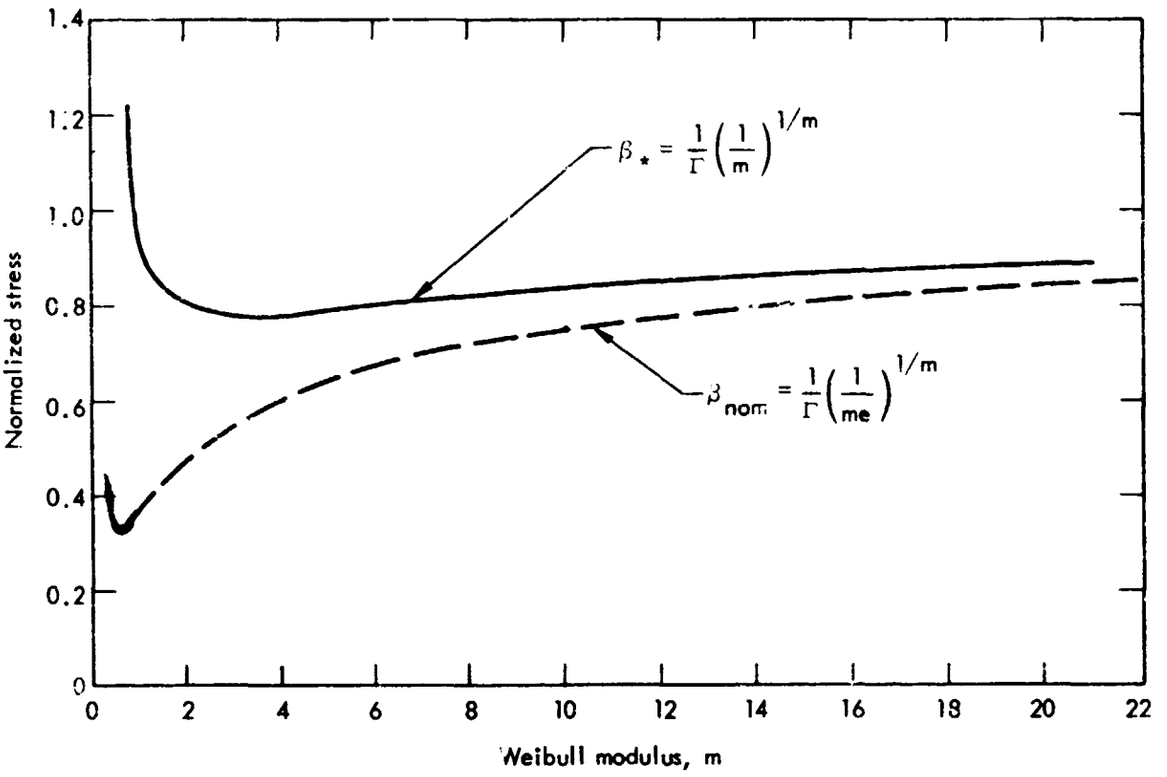

Fig. 20. Maximum filament stress, β_*, and nominal bundle strength, β_{nom}, both normalized to (i.e., divided by) average filament strength.

damage in fabrication, and other factors may bring the actual strength of a composite down to, or even below, the values predicted for the idealized, uniformly loaded free strand. The fabrication variables controlling composite strength are many and very often quite subtle, requiring a specific evaluation of a particular composite for characterization. The computations described earlier in this section should serve as a guide to what may reasonably be expected. As a thumb-rule example, a well-designed fiber composite with filaments having a trength distribution with m = 10 should have a nominal strength around

50% of the filament average strength (with 70% or so of the volume occupied by filaments). On the other hand, it will be an unusual composite which exhibits a nominal strength as high as 70 or 75% of the average filament strength.

The bundles illustrated in Fig. 19 can be evaluated analytically by Eq. (30). The comparisons are:

Bundle No.	Nominal Strength	Predicted Strength
1	6.8	6.4
2	7.5	7.0

When the applied load is nonuniform, as in flexure of a composite beam, the fact that only part of the filaments are highly loaded results in early fracture. This is an example of the adage, "united they stand, divided they fall." All of us take advantage, at least implicitly, of this principle (divide and conquer) when we tear cloth. Statistical analysis shows that the resistance of a multifilament strand to a linearly varying tension may be less than half of its capacity under uniform loading.

4. STRENGTH RETENTION OF DAMAGED MULTIFILAMENT STRANDS

Generally speaking, some fraction of the weakest filaments in the ideal strand fail before the ultimate capacity is reached. Therefore, a certain amount of internal fracture is tolerated without impairment of strand capacity. If, somehow, progressive severing of filaments occurred beyond this level, the capacity of the strand would decrease. If the strength distribution is approximately unimodal, the strength

retention of a strand will be (in normalized form)

$$\eta_{retained} = \eta\, S(\eta) \qquad (31)$$

where the fraction intact S is less than the critical fraction $S(\eta_*)$. For convenience we define a strength retention ratio as the ratio of retained strength to maximum strand capacity (using Eq. (25)):

$$R = \frac{\eta\, S(\eta)}{\eta_*\, S(\eta_*)} . \qquad (32)$$

If S is taken as a Weibull distribution we can write η in terms of S,

$$\eta = \left(\frac{ln \frac{1}{S}}{ln \frac{1}{S_p}} \right)^{1/m} ,$$

and the strength retention ratio becomes

$$R = \left(me\, ln \frac{1}{S} \right)^{1/m} S . \qquad (33)$$

The S-term in this equation (the fraction surviving) is an index of the degree of progressive damage among the weakest filaments of the strand. This equation is plotted in Fig. 21

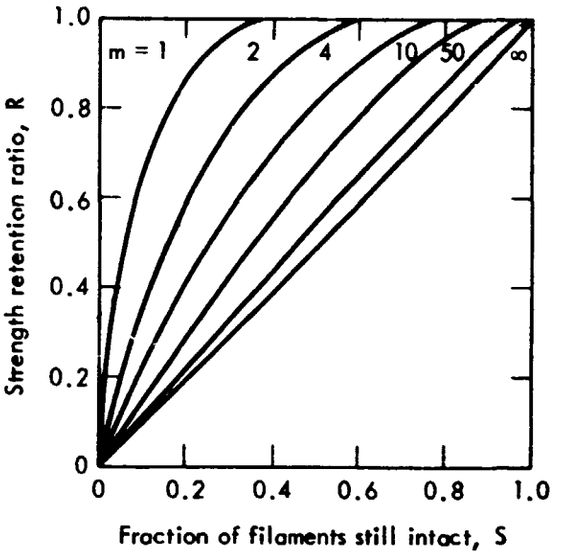

Fig. 21. Strength retention of progressively damaged strands, based on Weibull distribution. The strength retention ratio, R, is the ratio of remaining capacity to maximum capacity.

VII. ESTIMATION OF WEIBULL PARAMETERS FOR ORGANIC FIBER COMPOSITE (PRD/EPOXY) STRANDS

Large sample sizes of PRD/epoxy strands are being tested as part of a NASA sponsored program at the Lawrence Livermore Laboratory. Results of this test program are being reported in the progress reports under Contract C-13980-C and in the literature*. Figures 22 and 23 present a series of tensile strength measurement on single-end (280-filament)

*Chiao, T. T. and Moore, R. L., "Strength of an Organic Fiber in an Epoxy Matrix," UCRL Preprint - 74051.

composite strands. Figure 22 gives the first 120 measured values. This particular phase of the program was completed with a total of 484 tests, shown in Fig. 23. Weibull distribution functions with m = 25 and m = 20 are shown through the data. The functional fits are quite good over most of the data and are consistent with the skewness which prevails in both samples. The Weibull modulus estimates in these cases were obtained by plotting data onto the median-normalized chart of Fig. 7. Single point estimates, as described in Sec. III, showed the utility of these quick methods.

Table 7 presents various single-point estimators of Weibull modulus, as well as the value chosen from the graphical median plot.

Table 7

WEIBULL MODULUS FOR PRD 49/EPOXY STRANDS

Method	Figure 22 Data	Figure 23 Data
Least Value	15 *	18 *
Max. Value	25	25 **
Range	18 *	20
Coeff. of Var.	25	20
Median Plot	25	20

* Conservative at the minimum values

** Nonconservative at the minimum values

The table illustrates the value of several rapid estimators to yield a functional form which gives a reasonable fit to the data.

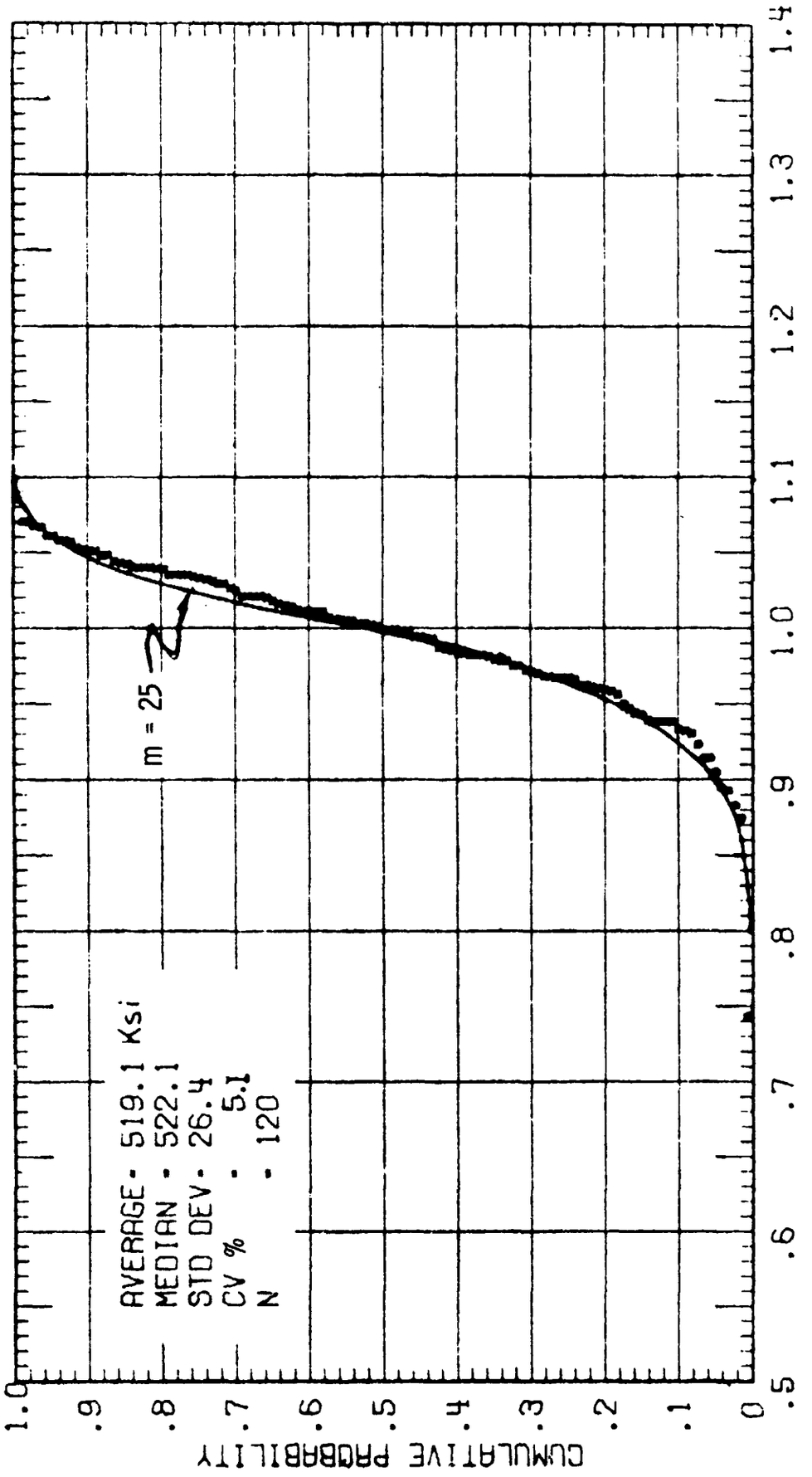

Fig. 22. Strength variation in PRD 49-III/epoxy strands.

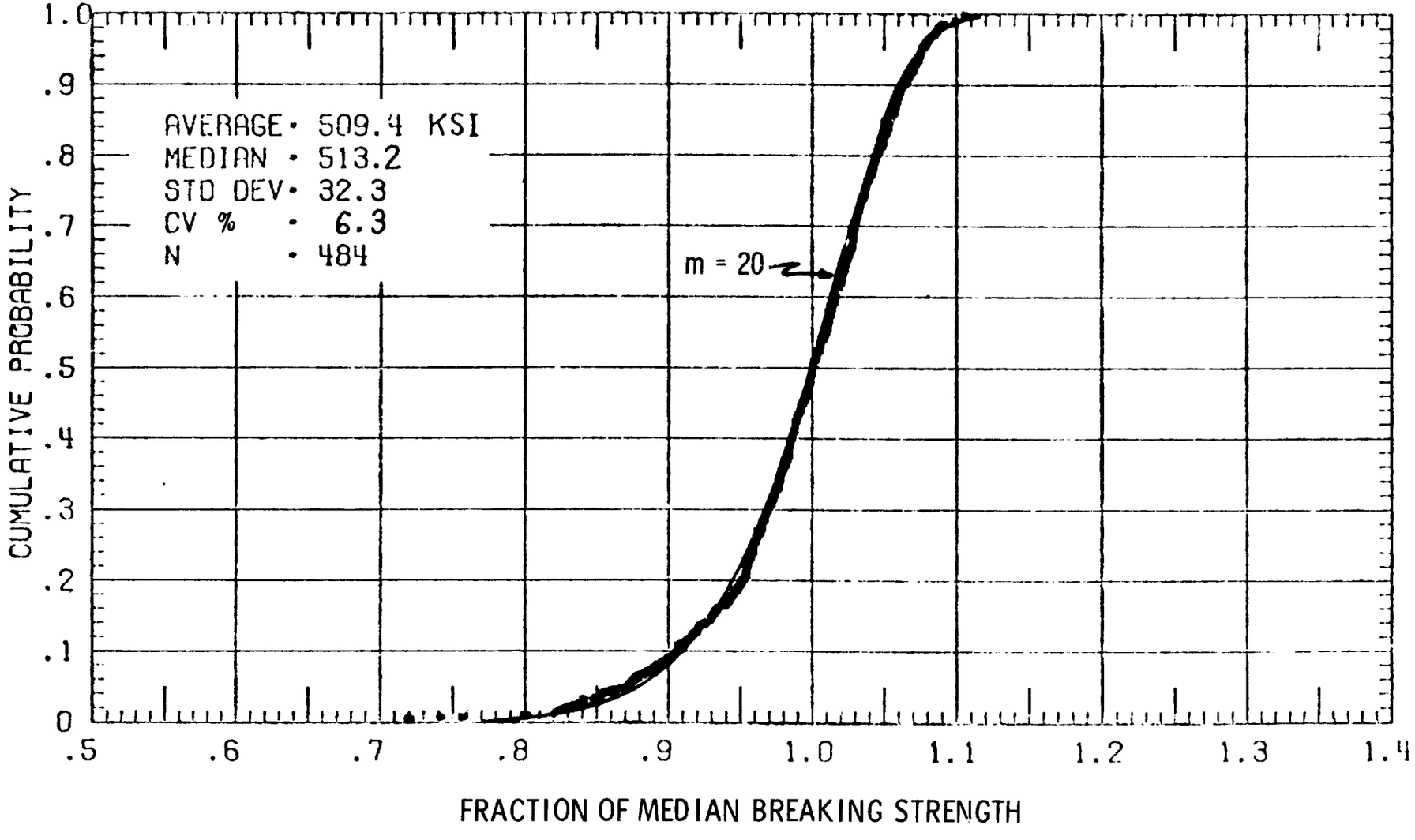

Fig. 23. Strength variation in PRD 49-III/epoxy strands.

It is significant that in both samples the Weibull moduli estimated by the least values were well below other single-point estimates. These data suggest an overall downward shift of properties from the results of the first 120 to the sample of 484. In addition to this shift, the isolated minimum value of Fig. 22 is reflected in the grouping of three low values shown in Fig. 23. There is a possibility of a distinct second mode in the population, located around 0.75 and representing about 1% of the population. Such a mode may be very crucial in reliability estimates.

The deviations between the Weibull distribution shown in Figs. 22 and 23 and the location of the observed least values were estimated by inverting Eq. (16) and using the median rank probability assignment:

$$\lambda_r = \left[\frac{\ln\left(\frac{N + 0.4}{N + 0.7 - r}\right)}{\ln(2)}\right]^{1/m}$$

and comparing the predicted values of λ with the observed values, as shown in Table 8.

The negative deviation values correspond to over-estimates of strength and contribute to suspicion of least-value behavior.

It is interesting to apply the size effect of Eq. (17) to these data. The most probable minimum values of ideal samples are related by $N^{1/m}$. Using the first (120) sample with m = 25 as a basis, the predicted least value in the second sample (484) is 368 ksi, identical with the observed value.

It is not known at present whether the causes of the statistical

differences between these two data sets are material and process factors or testing and handling methods.

Table 8

DEVIATION BETWEEN PREDICTED AND OBSERVED

STRENGTH IN PRD 49/EPOXY SAMPLES

Rank	Predict. m = 25	Fig. 1 Obs.	Deviation	Predict. m = 20	Fig. 2 Obs.	Deviation
1	.824	.74	-0.08	0.73	.72	-0.01
2	.855	.875	+0.02	.775	.742	-0.03
3	.871	.882	+0.01	.796	.758	-0.04
4	.882	.892	+0.01	.808	.8	-0.
5	.891	.895	+0.004	.815	.82	-0.

VIII. CONCLUSION

We have reviewed some statistical models that attempt to explain both the variability and the size dependence of the ultimate strength of brittle and fibrous materials. Specific calculations were carried out using the Weibull distribution to describe local weakness of the material. Experience has shown this distribution to have wide applicability, and it has consequently become a tool in diverse fields. In addition to interpreting strength, it has been used in studying fatigue, stress rupture, meteorology, gust loading, and other areas where extreme values are of interest. It has also demonstrated some definite shortcomings, particularly in the magnitude of the size effect prediction. In most studies of size effect the observed strength changes are not as great as predicted by the Weibull model. This feature is useful for scale-up or in fiber-reinforced structure since predictions will tend to be conservative; however, they may sometimes be too conservative to be tolerable.

The methods and graphs presented should facilitate processing, plotting, and fitting observations with the "best" two-parameter Weibull distribution and provide, at a glance, a perspective of least-value behavior. The application to redundant parallel systems of brittle elements (multifilament strands) produced some realistic bounds on the strength that might be achieved in a composite and indicated the degree of optimism which may be contained in the "law of mixtures."

The statistical approach is basically a local fracture model which, in conjunction with analysis of stress distribution, can lead to a statistical conclusion regarding a structure's reliability. It is,

therefore, a logical supplement to elastic stress analysis when variability of conventionally measured properties is dangerously large.

Application of the methods and charts was demonstrated on recent organic-fiber composite data and illustrated the utility of the Weibull distribution as well as possible problems which might be associated with infrequent second modes.

NASA — JPL — Coml., L.A., Calif.